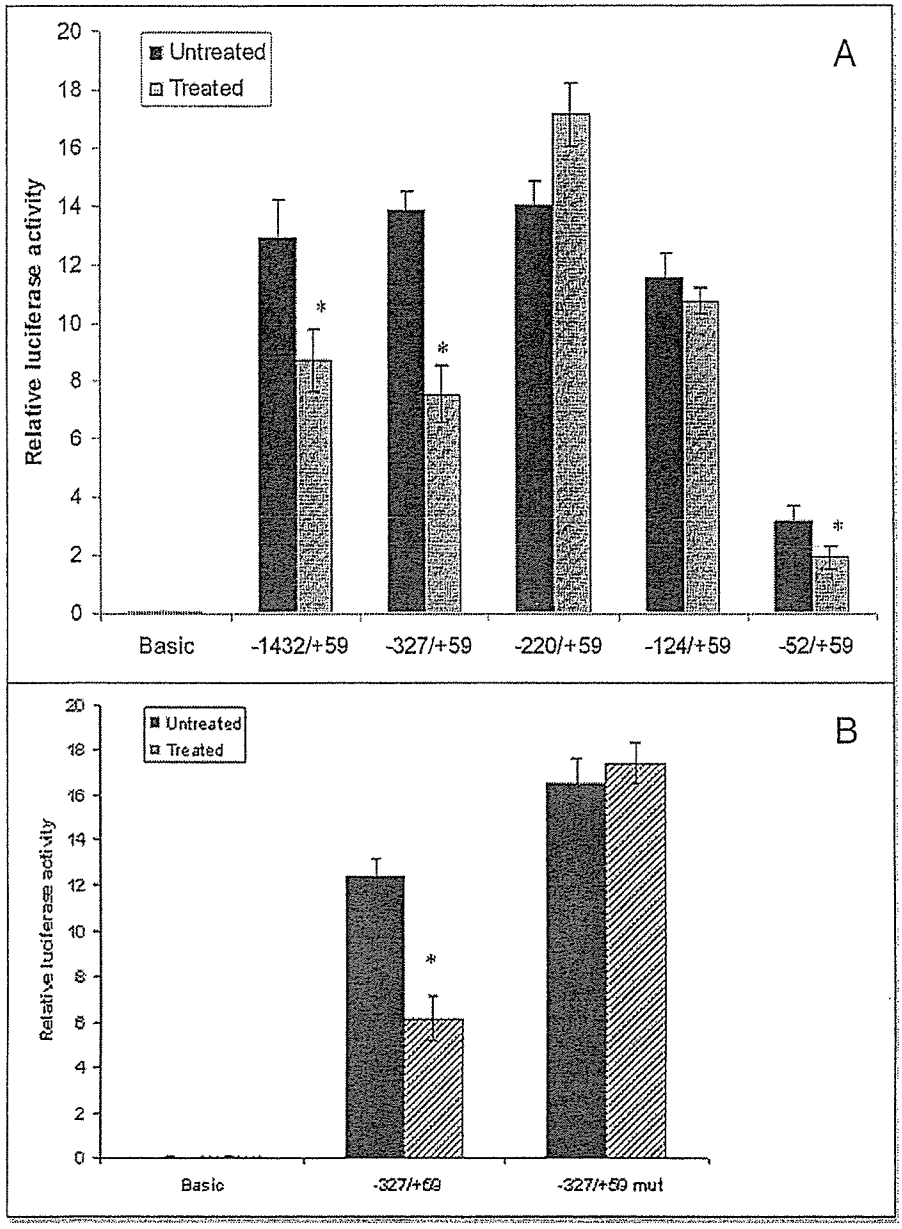

Figure 2. Transcriptional activity of COX-2 promoter constructs in HCA-7 cells treated with Se-Met at 90 μM. (A) HCA-7 cells were transfected with 0.5 μg of each COX-2 promoter construct for 24 h followed by Se-Met treatment for 12 h. Firefly and renilla luciferase activities were measured using Dual luciferase assay system (Promega). Firefly luciferase values were normalized to Renilla values. Mean ± S.E. of three independent experiments was plotted. (B) -327/+59 construct with a mutation in the NF-kB binding site was transfected into the HCA-7 cells for 24 h, followed by Se-Met treatment for 12 h. Data shown is derived from three independent experiments.

Deletion of NF-IL6 and CRE sites in -124/+59 and -52/+59 constructs resulted in a decrease of luciferase activity by 18% and 77%, respectively compared to -220/+59. These observations suggest that NF-IL6, and CRE element play an important role in regulating COX-2 transcription in HCA-7 cells. When transfected HCA-7 cells were treated with 90 μM Se-Met, -1432/+59 and -327/+59 constructs showed a significant ($P<0.05$) decrease in their luciferase activity by 33% and 46%, respectively compared to their untreated controls. No difference was seen in luciferase activity between control and Se-Met treatment with -220/+59 and -124/+59 COX-2 promoter constructs. These results indicate that Se-Met regulates COX-2 expression at transcriptional level possibly by targeting NF-κB.

To confirm the involvement of NF-κB transcription factor in Se-Met mediated COX-2 regulation, HCA-7 cells were transfected with -327/+59 construct carrying a mutation in NF-κB binding site. If Se-Met targets only NF-κB, no difference could be seen in luciferase activity between control and Se-Met treatment. The data in Figure 2B shows no decrease in luciferase activity with Se-Met treatment. Together, these observations suggest a role for NF-κB in the regulation of COX-2 by Se-Met.

Se-Met inhibits NF-κB DNA binding. Based on the observations from transfection experiments, we speculated that modulation of DNA binding of NF-κB by Se-Met could explain the observed decrease in luciferase activity in COX-2 promoter constructs that contains NF-κB binding sites in HCA-7 cells. We performed EMSA to examine binding of NF-κB using 32p-labeled consensus NF-κB double stranded oligonucleotides in both control and Se-Met 90 μM treated cells. NF-κB DNA binding was seen only with wild-type NF-κB oligonucleotides (Lane 2, Fig. 3), but not with mutant oligos (lane 5, Fig. 3). NF-κB binding was observed when labeled wild type-NF-κB oligonucleotides were incubated with nuclear extracts isolated from untreated HCA-7 cells (lane 2, Fig. 3), whereas this binding was completely inhibited in Se-Met treated HCA-7 cells (lane 3, Fig. 3). NF-κB binding was completely abrogated when the control nuclear extracts were incubated with an excess of nonlabeled wild type oligonucleotide (100x) for 30 min prior to the addition of labeled oligonucleotide (lane 4, Fig. 3), which clearly shows the specificity of the NF-κB binding. However, addition of nonlabeled mutant oligonucleotide had no effect on the binding (lane 6, Fig. 3).

NF-κB exists in the form of either homo- or heterodimer composed of five different subunits. To identify the subunits of NF-κB involved in this binding, super-shift analysis was carried out by incubating the nuclear extracts with anti-p65- and anti-p50 antibodies. The binding complex was super-shifted only with p65 antibody but not with p50 (lanes 7 and 8, Fig. 3). Together these observations suggested that Se-Met treatment inhibits DNA binding of p65 subunit of NF-κB.

Decreased nuclear translocation of NF-κB/p65 with Se-Met treatment. In its inactive form, NF-κB is predominantly located in cytoplasm and bound to inhibitory IkB proteins. Degradation of these IkBs by phosphorylation at serine residues by upstream kinases results in release of NF-κB, which then translocates into the nucleus and activates its target genes. To determine whether inhibition of NF-κB DNA binding with Se-Met treatment is due to reduced nuclear accumulation of NF-κB/p65, western

analysis was carried out with nuclear extracts isolated from untreated and cells treated with Se-Met at 60 (IC_{50} dose) and 90 μM. Se-Met treatment resulted in dose-dependent reduction of NF-κB/p65 nuclear accumulation in HCA-7 cells (Fig. 4).

DISCUSSION

Dietary selenium supplementation with selenium-enriched yeast has been shown to be associated with marked reduction in the risks for developing prostate, lung, and colorectal cancer.[13] Currently, selenium alone or in combination with other chemopreventive agents is being evaluated in clinical trials against human colon and prostate cancers.[23,24] However, the molecular and cellular effects of selenium underlying its anti-cancer effects are not completely understood. Se-Met is an organic form of selenium present in a variety of natural foods and is being identified as a predominant form of Se in selenized yeast.[25] Previous in vitro studies have shown that Se-Met inhibits COX-2 expression in colon cancer cells.[15] However, whether COX-2 inhibition by Se-Met occurs at transcriptional or post-transcriptional level is not known. In the present study, we demonstrate that Se-Met significantly inhibits luciferase activity of COX-2 reporter constructs. This suggests that Se-Met inhibits COX-2 at the transcriptional level.

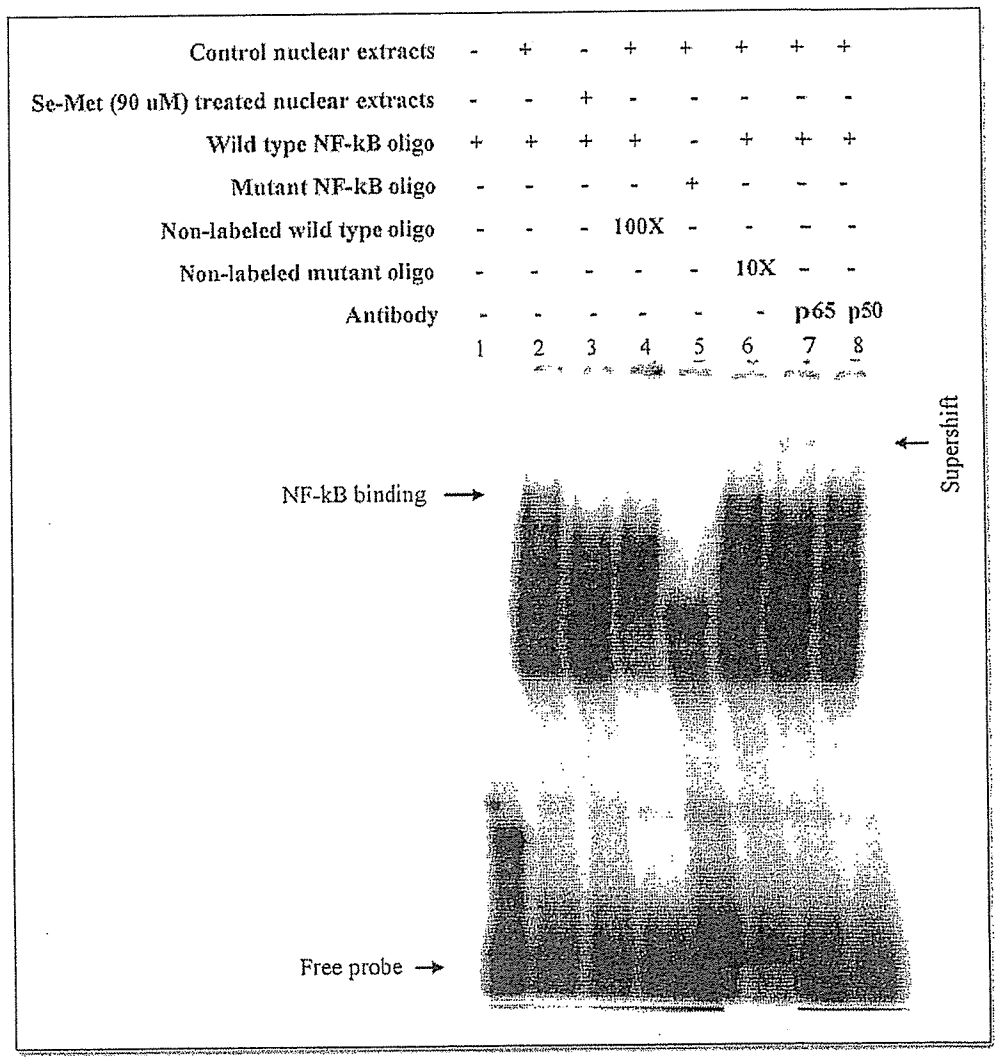

Figure 3. Effect of Se-Met on NF-kB DNA binding in HCA-7 cells. Cells were treated with 90 μM Se-Met for 6 days and nuclear extracts were prepared. EMSA was performed with 10 μg of nuclear proteins which were incubated with 32p-labeled double stranded NF-kB consensus oligonucleotide for 30 min. NF-kB binding complexes were analyzed by supershift analysis using anti-p65 and 50 antibodies. The data shown is a representative of the three experiments and similar results were observed in all the three experiments.

COX-2 promoter constructs using luciferase as a reporter gene were described in previous studies.[26,27] The COX-2 reporter construct -327/+59 showed slightly higher luciferase activity compared to that of -1432/+59 in HCA-7 cells. This observation suggests that -327/+59 region that contains consensus sequences for NF-κB site, NF-IL6 site, and CRE is sufficient for the induction of COX-2 transcription. Further, reduction in luciferase activity observed with the deletion of NF-IL6 site, and CRE indicate key role of these cis-acting elements in regulating COX-2 transcription. These data is consistent with the previous studies.[17,27] Post-transcriptional mechanisms also appears to be important for the sustained induction of COX-2.[17] Interestingly, Se-Met treatment at 90 μM significantly reduced the luciferase activity of those reporter constructs that contain binding sites for NF-κB. These data demonstrate that Se-Met inhibits COX-2 at transcriptional level by selectively targeting NF-κB transcription factor. These findings were further supported by using -327/+59 reporter construct with a mutation in NF-κB binding site in which Se-Met treatment did not alter the luciferase activity.

Electrophoretic mobility shift assays using double-stranded NF-κB consensus oligonucleotides showed that Se-Met completely inhibits NF-κB DNA binding in HCA-7 cells. This observation is consistent with previous studies using other selenium compounds in different cell types.[21,28-31] Competition experiments with an excess of nonlabeled wild type and mutant oligos showed binding specificity of NF-κB. Supershift analysis by incubating nuclear protein extracts with anti-p65 and p50 antibodies identified the presence of p65 protein but not p50, suggesting that Se-Met inhibits DNA binding of NF-κB/p65 protein. These results can be explained by the observed reduction in nuclear translocation of NF-κB/p65 by Se-Met

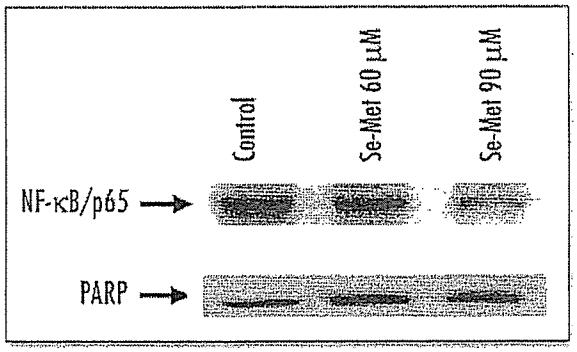

Figure 4. Se-Met inhibited nuclear translocation of NF-kB/p65 in HCA-7 colon cancer cells. Cells were treated with 60 & 90 μM Se-Met for 6 days, and the nuclear protein extracts were prepared. 50 μg of nuclear protein was separated on SDS-PAGE, transferred to nylon membrane, and probed with goat polyclonal anti-NFkB/p65 overnight. The experiment was repeated twice and similar results were observed. PARP was used as a loading control.

and this reduction is dose-dependent at 60 and 90 μM of Se dose. The molecular mechanisms by which Se-Met inhibits NF-κB activation requires further study. One possible mechanism could be inhibiting phosphorylation of IkB proteins by their upstream IKK kinases and thereby preventing their degradation as observed with some selenium compounds in prostate cancer cells.[30]

In this current study, we observed maximum inhibition of NF-κB by Se-Met at doses that are higher than the concentration seen in previous clinical trials.[13] However, our findings are supported by a recent study in which Se-Met maximally inhibited nuclear accumulation of NF-κB/p65, as measured by flow cytometric analysis, in peroxynitrite- and LPS-challenged leukocytes and polymorphonuclear cells at 100 μM dose.[32] Furthermore, it has been reported that prolonged periods of Se supplementation with 750–850 μg may not be associated with any adverse side effects.[33] Also in type II diabetic patients extra daily supplementation of Se at 960 μg (Se group) decreased the NF-κB/p65 DNA binding to the control levels (non-diabetic group) with no observed toxicity symptoms of Se.[31] Finally, it is worth noting that toxicity profile in high dose selenium supplementation conducted in men with biopsy-proven prostate cancer who were randomized to either 1600 or 3200 μg/day of selenized yeast suggest that doses greater than 400 μg/day could be given in controlled conditions for an extended period of time, without serious toxicity.[34]

In summary, our findings demonstrate that Se-Met inhibits COX-2 at transcriptional level by modulating NF-κB activation. These observations holds significance in light of a recent immunohistochemical study that showed elevated levels of NF-κB and further coexpression of NF-κB and COX-2 in moderately and well-differentiated colonic malignant epithelial cells, indicating the possibility of NF-κB mediated COX-2 induction in these cells.[35] In this context, Se-Met supplementation may be useful in suppression of COX-2 and its downstream effects by inhibiting NF-κB pathway in colorectal cancer.

References

1. Eberhart CE, Coffey RJ, Radhika A, Giardiello FM, Ferrenbach S, DuBois RN. Upregulation of cyclooxygenase-2 expression in human colorectal adenomas and adenocarcinomas. Gastroenterology 1994; 107:1183-8.
2. Khan KN, Masferrer JL, Woerner BM, Soslow R, Koki AT. Enhanced cyclooxygenase-2 expression in sporadic and familial adenomatous polyposis of the human colon. Scand J Gastroenterol 2001; 36:865-9.
3. Einspahr JG, Krouse RS, Yochim JM, Danenberg PV, Danenberg KD, Bhattacharya AK, Martinez ME, Alberts DS. Association between cyclooxygenase expression and colorectal adenoma characteristics. Cancer Res 2003; 63:3891-3.
4. Kojima M, Morisaki T, Izuhara K, Uchiyama A, Matsunari Y, Katano M. Lipopolysachharide increases cyclooxygenase-2 expression in a colon carcinoma cell line through nuclear factor-kB activation. Oncogene 2000; 19:1225-31.
5. Liu W, Reinmuth N, Stoelzing O, Parikh AA, Tellez C, Williams S, Jung YD, Fan F, Takeda A, Akagi M, Bar-Eli M, Gallick GE, Ellis LM. Cyclooxygenase-2 is upregulated by interleukin-1β in human colorectal cancer cells via multiple signaling pathway. Cancer Res 2003; 63:3632-6.
6. Oshima M, Dinchuk JE, Kargman S, Oshima H, Hancock B, Kwong E. Suppression of intestinal polyposis in Apc delta716 knockout mice by inhibition of cyclooxygenase 2 (COX-2). Cell 1996; 87:803-9.
7. Liu CH, Chang SH, Narko K, Trifan OC, Wu MT, Smith AE, Haudenschild C, Lane TF, Hla T. Overexpression of cyclooxygenase-2 is sufficient to induce tumorigenesis in transgenic mice. J Biol Chem 2001; 276:18563-9.
8. Tsujii M, Kawano S, Tsuji S, Sawaoka H, Hori M, DuBois RN. Cyclooxygenase regulates angiogenesis induced by colon cancer cells. Cell 1998; 93:705-16.
9. Chen WS, Wei SJ, Liu JM, Hsiao M, Kou-Lin J, Yang WK. Tumor invasiveness and liver metastasis of colon cancer cells correlated with cyclooxygenase-2 (COX-2) expression and inhibited by a COX-2-selective inhibitor, Etodolac. Int J Cancer 2001; 91:894-9.
10. Sheng H, Shao J, Washington MK, DuBois RN. Prostaglandin E2 increases growth and motility of colorectal carcinoma cells. J Biol Chem 2001; 276:18075-81.
11. Pai R, Nakamura T, Moon WS, Tarnawski AS. Prostaglandins promote colon cancer cell invasion; signaling by cross-talk between two distinct growth factor receptors. FASEB J 2003; 17:1640-7.
12. Gupta RA, DuBois RN. Colorectal cancer prevention and treatment by inhibition of cyclooxygenase-2. Nat Rev Cancer 2001; 1:11-21.
13. Clark LC, Combs GF Jr, Turnbull BW, Slate EH, Chalker DK, Chow J, Davis LS, Glover RA, Graham GF, Gross EG, Krongrad A, Lesher JL Jr, Park HK, Sanders BB Jr, Smith CL, Taylor JR. Effects of selenium supplementation for cancer prevention in patients with carcinoma of the skin. A randomized controlled trial. Nutritional prevention of cancer study group. JAMA 1996; 276:1957-63.
14. Redman C, Scott JA, Baines AT, Basye JL, Clark LC, Calley C, Roe D, Payne CM, Nelson MA. Inhibitory effect of selenomethionine on the growth of three selected human tumor cell lines. Cancer Lett 1998; 125:103-10.
15. Baines A, Taylor-Parker M, Goulet AC, Renaud C, Gerner EW, Nelson MA. Selenomethionine inhibits growth and suppresses cyclooxygenase-2 (COX-2) protein expression in human colon cancer cell lines. Cancer Biol Ther 2002; 114:374-8.
16. Kutchera W, Jones DA, Matsunami N, Groden J, McIntyre TM, Zimmerman GA, White RL, Prescott SM. Prostaglandin H synthase 2 is expressed abnormally in human colon cancer: Evidence for a transcriptional effect. Proc Natl Acad Sci USA 1996; 93:4816-20.
17. Shao J, Sheng H, Inoue H, Morrow JD, DuBois RN. Regulation of constitutive cyclooxygenase-2 expression in colon carcinoma cells. J Biol Chem 2000; 275:33951-6.
18. Zhang Z, Sheng H, Shao J, Beauchamp RD, DuBois RN. Posttranscriptional regulation of cyclooxygenase-2 in rat intestinal epithelial cells. Neoplasia 2000; 2:523-30.
19. Tazawa R, Xu XM, Wu KK, Wang LH. Characterization of the genomic structure, chromosomal location and promoter of human prostaglandin H *synthase-2* gene. Biochem Biophys Res Commun 1994; 203:190-9.
20. Araki Y, Okamura S, Hussain SP, Nagashima M, He P, Shiseki M, Miura K, Harris CC.. Regulation of cyclooxygenase-2 expression by the Wnt and Ras pathways. Cancer Res 2003; 63:728-34.
21. Zamamiri-Davis F, Lu Y, Thompson JT, Prabhu KS, Reddy PV, Sordillo LM, Reddy CC.. Nuclear factor-kB mediates overexpression of cyclooxygenase-2 during activation of RAW 264.7 macrophages in selenium deficiency. Free Radical Biol Med 2002; 32:890-7.
22. Subbaramaiah K, Cole PA, Dannenberg AJ. Retinoids and carnosol suppress cyclooxygenase-2 transcription by CREB-binding protein/p300-dependent and -independent mechanisms. Cancer Res 2002; 62:2522-30.
23. Frank DH, Roe DJ, Sherry Chow HH, Guillen JM, Choquette K, Gracie D, Francis J, Fish A, Alberts DS. . Effects of a high-selenium yeast supplement on celecoxib plasma levels: A randomized phase II trial. Cancer Epidemiol Biomark Prev 2004; 13:299-303.
24. Pak RW, Lanteri VJ, Scheuch JR, Sawczuk IS. Review of vitamin E and selenium in the prevention of prostate cancer: Implications of the selenium and vitamin E chemoprevention trial. Integrated Cancer Ther 2002; 1:338-44.
25. Block E, Glass RS, Jacobsen NE, Johnson S, Kahakachchi C, Kaminski R, Skowronska A, Boakye HT, Tyson JF, Uden PC. Identification and synthesis of a novel selenium-sulfur amino acid found in selenized yeast: Rapid indirect detection NMR methods for characterizing low-level organoselenium compounds in complex matrices. J Agric Food Chem 2004; 52:3761-71.

26. Inoue H, Nanayama T, Hara S, Yokoyama C, Tanabe T. The cAMP response element plays an essential role in the expression of the human prostaglandin-endoperoxide *synthase-2* gene in differentiated in U937 monocytic cells. FEBS Lett 1994; 350:51-4.
27. Inoue H, Yokoyama C, Hara S, Tone Y, Tanabe T. Transcriptional regulation of human prostaglandin-endoperoxide *synthase-2* gene by lipopolysachharide and phorbol ester in vascular endothelial cells. Involvement of both nuclear factor for interleukin-6 expression site and cAMP response element. J Biol Chem 1995; 270:24965-71.
28. Kim IY, Stadtman TC. Inhibition of NF-κB DNA binding and nitric oxide induction in human T cells and lung adenocarcinoma cells by selenite treatment. Proc Natl Acad Sci USA 1997; 94:12904-7.
29. Prabhu KS, Zamamiri-Davis F, Stewart JB, Thompson JT, Sordillo LM, Reddy CC. Selenium deficiency increases the expression of inducible nitric oxide synthase in RAW 264.7 macrophages: Role of nuclear factor-kB in upregulation. Biochem J 2002; 366:203-9.
30. Gasparian AV, Yao YJ, Lu J, Yemelyanov AY, Lyakh LA, Slaga TJ, Budunova IV. Selenium compounds inhibit IkB kinase (IKK) and nuclear factor-kB (NF-κB) in prostate cancer cells. Mol Cancer Ther 2002; 1:1079-87.
31. Faure P, Ramon O, Favier A, Halimi S. Selenium supplementation decreases nuclear factor-kappa B activity in peripheral blood mononuclear cells from type 2 diabetic patients. Eur J Clin Invest 2004; 34:475-81.
32. Jozsef L, Filep JG. Selenium-containing compounds attenuate peroxynitrite-mediated NF-κB and AP-1 activation and *interleukin-8* gene and protein expression in human leukocytes. Free Radical Biol Med 2003; 35:1018-27.
33. Yang G, Yin S, Zhou R, Gu L, Yan B, Liu Y, Liu Y. Studies of safe maximal daily dietary Se-intake in a seleniferous area in China. Part II: Relation between Se-intake and the manifestation of clinical signs and certain biochemical alterations in blood and urine. J Trace Elem Electrolytes Health Dis 1989; 3:123-30.
34. Reid ME, Stratton MS, Lillico AJ, Fakih M, Natarajan R, Clark LC, Marshall JR. A report of high-dose selenium supplementation: response and toxicities. J Trace Elem Med Biol 2004;18:69-74.
35. Charalambous MP, Maihofner C, Bhambra U, Lightfoot T, Gooderham NJ. The colorectal cancer study group. Upregulation of cyclooxygenase-2 is accompanied by increased expression of nuclear factor-kB and IkB kinase- in human colorectal cancer epithelial cells. Br J Cancer 2003; 88:1598-604.

Long-Term and Sustained COMP-Ang1 Induces Long-Lasting Vascular Enlargement and Enhanced Blood Flow

Chung-Hyun Cho, Kyung Eun Kim, Jonghoe Byun, Hyung-Suk Jang, Duk-Kyung Kim, Peter Baluk, Fabienne Baffert, Gyun Min Lee, Naoki Mochizuki, Jin Kim, Byeong Hwa Jeon, Donald M. McDonald, Gou Young Koh

Abstract—Vascular enlargement is a characteristic feature of angiopoietin-1 (Ang1)-induced changes in adult blood vessels. However, it is unknown whether tissues having Ang1-mediated vascular enlargement have more blood flow or whether the enlargement is reversible. We have recently created a soluble, stable and potent Ang1 variant, COMP-Ang1. In the present study, we investigated the effects of varied dose and duration of COMP-Ang1 on vascular enlargement and blood flow in the tracheal microvasculature of adult mice and explored a possible mechanism of long-lasting vascular enlargement. We found that COMP-Ang1 administered by adenoviral vector induced long-lasting vascular enlargement and increased tracheal blood flow. In contrast, short-term administration of COMP-Ang1 recombinant protein induced transient vascular enlargement that spontaneously reversed within a month. In both cases, the vascular enlargement resulted from endothelial proliferation. The COMP-Ang1–induced vascular remodeling is mediated mainly through Tie2 activation. Sustained overexpression of Tie2 could participate in the maintenance of vascular changes. Together, our findings indicate that sustained treatment with COMP-Ang1 can produce long-lasting vascular enlargement and increased blood flow. (*Circ Res.* **2005;97:86-94.**)

Key Words: angiopoietin-1 ■ COMP-Ang1 ■ vascular enlargement ■ blood flow

Angiopoietin-1 (Ang1) is known to be a ligand to Tie2 tyrosine kinase receptor expressed on endothelial cells.[1] Ang1/Tie2 signaling is thought be involved in branching and remodeling of the primitive vascular network and in the recruitment of mural cells during development.[2,3] Transgenic overexpression of Ang1 using the skin-specific keratin-14 promoter produces leakage-resistant and enlarged vessels with an increased number of endothelial cells in skin.[4,5] Gene transfer of Ang1 into ischemic tissues produces notably enlarged blood vessels.[6,7] Baffert et al recently identified that Ang1-induced vascular enlargement could be the result of endothelial proliferation in trachea mucosa.[8] Thus, a cardinal feature of Ang1-induced vascular remodeling is vascular enlargement resulting from endothelial cell proliferation in adult animals.[4–8]

Given that Ang1-induced therapeutic benefits correlated with vascular enlargement in the ischemic tissues,[6,7,9] enhanced blood flow through blood vessels enlarged by Ang1 treatment could provide a great therapeutic benefit to ischemic peripheral tissues. However, it is not known whether the tissues having Ang1-mediated enlarged vessels have more blood flow. In addition, the effective dose and treatment period of Ang1 for inducing effective vascular enlargement is not known. Moreover, it is not known whether Ang1-mediated vascular enlargement regresses when Ang1 stimulation is withdrawn.

We have recently developed a soluble, stable, and potent Ang1 variant, COMP-Ang1.[10] To create this protein, we replaced the amino-terminal portion of Ang1 with the short coiled-coil domain of cartilage oligomeric matrix protein (COMP). COMP-Ang1 is more potent than native Ang1 in phosphorylating the Tie2 receptor and signaling via Akt in primary cultured endothelial cells.[10]

In the present study, we investigated effects of period and dose of COMP-Ang1 on vascular enlargement and tissue blood flow in adult mice and investigated a possible mechanism for long-lasting vascular enlargement induced by long-term and sustained COMP-Ang1. To determine the underly-

Original received March 29, 2005; resubmission received May 10, 2005; revised resubmission received June 8, 2005; accepted June 8, 2005.

From the Biomedical Research Center and Department of Biological Sciences (C.-H.C., K.E.K., G.M.L., G.Y.K), Korea Advanced Institute of Science and Technology, Daejeon, Korea; the Department of Medicine (J.B., H.-S.J., D.-K.K.), Samsung Medical Center and Samsung Biomedical Research Institute, Sungkyunkwan University School of Medicine, Seoul, Korea; the Cardiovascular Research Institute, Comprehensive Cancer Center, and Department of Anatomy (P.B., F.B., D.M.M.), University of California, San Francisco; the Department of Structural Analysis (N.M.), National Cardiovascular Center Research Institute, Suita, Osaka, Japan; the Department of Anatomy (J.K.), College of Medicine, The Catholic University of Korea Seoul; and the Department of Physiology (B.H.J), College of Medicine, Chungnam National University Daejeon, Korea.

Correspondence to Gou Young Koh, Biomedical Research Center, Korea Advanced Institute of Science and Technology, 373-1, Guseong-dong, Daejeon, 305-701, Republic of Korea. E-mail gykoh@kaist.ac.kr

Circulation Research **is available at http://circres.ahajournals.org** **DOI: 10.1161/01.RES.0000174093.64855.a6**

ing mechanism of COMP-Ang1–stimulated vascular remodeling in adult mice, we focused on the microvasculature of the trachea, which is distinguished by its simplicity and monolayer structure. Our results indicate that long-term and sustained COMP-Ang1 produced by adenoviral delivery of COMP-Ang1 induces a long-lasting vascular enlargement and enhanced blood flow without enhanced pericyte recruitment in adult mice. Long-lasting Tie2 expression could be involved in the long-lasting vascular enlargement and enhanced blood flow.

Materials and Methods

Generation of COMP-Ang1 Recombinant Protein and Ade-COMP-Ang1

Recombinant Chinese hamster ovary cells expressing COMP-Ang1 (CA1–2; production rate, ≈30 mg/L) were established as previously described.[11] Recombinant adenovirus expressing COMP-Ang1 or LacZ was constructed using the pAdEasy vector system (Qbiogene). For additional Materials and Methods, see online data supplement at http://circres.ahajournals.org.

Animals, Treatment, and Measurement of Blood Pressure and Heart Rate

Specific pathogen-free FVB/N mice and Tie2-GFP transgenic mice (FVB/N)[12] were purchased from Jackson Laboratory and bred in our pathogen-free animal facility. Male mice 8 to 10 weeks old were used for this study. Animal care and experimental procedures were performed under approval from the Animal Care Committees of the Korea Advanced Institute of Science and Technology. For protein treatment, 200 μg of COMP-Ang1 recombinant protein or BSA dissolved in 50 μL of sterile 0.9% NaCl was injected daily through the tail vein for 2 weeks. For adenoviral treatment, the indicated amount of Ade-COMP-Ang1, Ade-LacZ, or Ade-sTie2-Fc (generous gift from Drs Gavin Thurston and Ella Ioffe at Regeneron Pharmaceuticals, Terrytown, NY) diluted in 50 μL of sterile 0.9% NaCl was injected intravenously through the tail vein. Systemic blood pressure and heart rate were measured under anesthesia.

Enzyme-Linked Immunosorbent Assay

Approximately 50 μL of blood was obtained from the tail vein into a heparinized capillary tube at the indicated times. ELISA was adopted for precise detection of COMP-Ang1 in plasma.

Immunohistochemical Staining

Mice were anesthetized, perfused with 1% paraformaldehyde in PBS, and several organs including tracheas were removed. Tracheas and ear skins were immunostained as whole mounts, whereas other organs were immunostained as sections. Signals were visualized, and digital images were obtained with a Zeiss Apotome microscope and a Zeiss LSM 510 confocal microscope.

Measurement of Tracheal Tissue Blood Flow

After the mice were anesthetized, a type N flowprobe (Transonic Systems Inc, Ithaca, NY) was placed on tracheal wall along second, third, and forth cartilage rings without applying pressure, as this would occlude the vessels and reduce perfusion in the area of interest. The flowprobe was kept in place on the position of the highest sensitivity by a micromanipulator and connected to a laser-Doppler flowmeter (model BLF21; Transonic Systems Inc), which can measure microcirculation in 1 mm^3 of tissue for real-time assessment of perfusion (mL/min per 100 g of tissue).

Morphometric Measurements and Statistics

Morphometric measurements of the vessel diameters and area densities in mouse trachea were made as previously described.[13] For each trachea, the numbers of PH3-immunopositive endothelial cells, platelet/endothelial cell adhesion molecule (PECAM)-1–immunopositive blood vessels, and desmin/NG2-immunopositive pericytes were measured in 5 regions, each 0.21 mm^2 in area. Values were expressed per millimeter squared. Values presented are mean±SD. Significance of differences between mean was tested by analysis of variance followed by the Student–Newman–Keuls test. Statistical significance was set at $P<0.05$.

Results

Systemic Adenoviral COMP-Ang1 Produces Differential Enlargements of Blood Vessels in Mouse Tracheal Mucosa

For in vivo treatments with COMP-Ang1, we developed a stable Chinese hamster ovary cell line (CA1–2) which produces COMP-Ang1 at ≈30 mg/L. The potency, solubility, oligomerization status, and stability of the COMP-Ang1 produced from CA1–2 are similar to those of COMP-Ang1 produced from COS-7 cells transiently transfected with plasmid vector containing the COMP-Ang1 gene[10] (data not shown). Adult mice were treated with a daily intravenous injection of 200 μg of COMP-Ang1 recombinant protein or BSA through the tail vein for 2 weeks, then blood vessels in the tracheal mucosa were visualized with PECAM-1 immunostaining (Figure 1). Six segments of the microvasculature were distinguished by their position in the vascular hierarchy and differences in endothelial cell morphology.[14] Enlargement of tracheal blood vessels was found in mice that received COMP-Ang1 in the following descending order of effect: postcapillary venules>capillaries>collecting venules>venules>terminal arterioles (Figure 1B). No significant change was noted in segmental arterioles. These phenomena were observed in all individuals of several mouse strains studied (FVB/N, C57BL/6, BALB/c, BALB/c-*nu*, C3H/HeJ). No changes in the sizes or shape of tracheal blood vessels were found in mice that received BSA.

Short-Term and Intermittent Circulating COMP-Ang1 Induces Reversible Enlargement of Postcapillary Venules and Arterioles in Tracheal Vessels

When 200 μg of COMP-Ang1 recombinant protein was injected intravenously into adult male mice, circulating COMP-Ang1 level peaked immediately after injection (≈3.75 minutes), then declined, and returned almost to the control level 3 to 4 hours after treatment (Figure 2A, left). The half-life ($t_{1/2}$) of circulating COMP-Ang1 was 11.8 minutes. Daily intravenous injection of 200 μg of COMP-Ang1 for 1 week in mice produced an ≈2.0-fold enlargement of postcapillary venules and a 1.4-fold enlargement of terminal arterioles in the trachea (Figure 2). The COMP-Ang1–induced enlargement of postcapillary venules, collecting venules, venous end of capillaries, venules, and terminal arterioles were further increased up to 2 weeks on continuation of daily injection of COMP-Ang1 for up to 2 weeks. However, COMP-Ang1–induced enlarged blood vessels returned gradually to normal after discontinuation of the COMP-Ang1 treatment (Figure 2). One month after discontinuation of the COMP-Ang1 treatment, a second round of treatment with a daily intravenous injection of 200 μg of COMP-Ang1 for 2 weeks induced similar enlargements

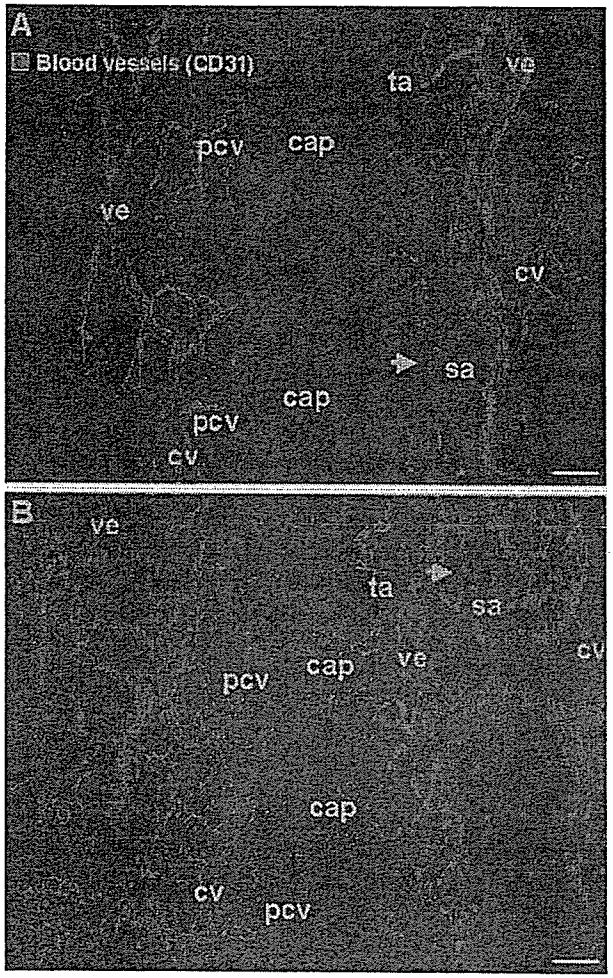

Figure 1. Effect of systemic COMP-Ang1 protein treatment on blood vessels in mouse tracheal mucosa. FVB/N mice were treated with daily injections of 200 μg of BSA (A) or 200 μg of COMP-Ang1 recombinant protein (B) for 14 days. Blood vessels in tracheal whole mounts were visualized with PECAM-1 (CD31) immunostaining (red). Six segments of the microvascular hierarchy are evident: segmental arteriole (sa, arrows), terminal arteriole (ta), capillary (cap), postcapillary venule (pcv), collecting venule (cv), and venule (ve). Of these, postcapillary venules and the venous ends of capillaries were the most enlarged after treatment by COMP-Ang1. The results from 4 experiments were similar. Scale bar=50 μm.

of tracheal vessels, again in a reversible manner (data not shown). In comparison, the diameters of tracheal vessels were indistinguishable between the control and experimental periods in tracheal vessels of mice treated with BSA (data not shown). These results indicate that short-term spikes of circulating COMP-Ang1 induce reversible enlargement of some tracheal vessels.

Long-Term and Sustained Circulating COMP-Ang1 Induces Long-Lasting Enlargement of Postcapillary Venules and Terminal Arterioles in Tracheal Vessels

As an alternative method for systemic treatment with COMP-Ang1, an adenoviral vector encoding the COMP-Ang1 gene (Ade-COMP-Ang1) was developed. As a control, an adeno-

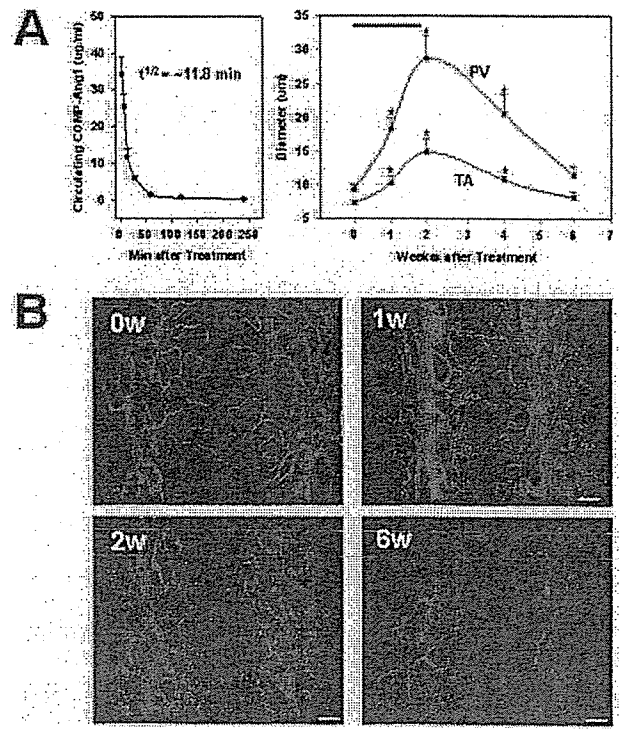

Figure 2. Effect of systemic COMP-Ang1 protein treatment on postcapillary venules and terminal arterioles. FVB/N mice were treated by daily injection of COMP-Ang1 recombinant protein (200 μg) for 14 days (A, black bar). At the indicated times, tracheal vessels were visualized with PECAM-1 immunostaining (B, red). The diameter of postcapillary venules and terminal arterioles are shown (A, right). Circulating plasma levels of COMP-Ang1 were measured by ELISA after a single injection of COMP-Ang1 recombinant protein (200 μg/mouse) (A, left). Diameters of 35 to 40 postcapillary venules (PV)/5 fields (brown curve) and 10 to 12 terminal arterioles (TA)/10 fields (blue curve) were measured at the edge of cartilage rings in each mouse. Values are mean±SD from 4 to 5 mice. *$P<0.05$ vs control period. COMP-Ang1 induced enlargement of postcapillary venules, collecting venules, venous ends of capillaries, venules, and terminal arterioles for up to 2 weeks, and then the enlarged blood vessels returned gradually to normal after discontinuation of the COMP-Ang1 treatment. Scale bar=50 μm.

viral vector encoding the LacZ gene (Ade-LacZ) was developed. The potency, solubility, oligomerization status, and stability of the COMP-Ang1 produced from HEK293 cells transduced with Ade-COMP-Ang1 are similar to that of COMP-Ang1 produced from COS-7 cells transiently transfected with plasmid vector containing the COMP-Ang1 gene[10] (data not shown). Adult mice were treated with 1×10^9 pfu Ade-COMP-Ang1 or Ade-LacZ. At multiple times more than a period of 16 weeks, circulating plasma COMP-Ang1 levels were measured, and blood vessels in tracheal mucosa were visualized with PECAM-1 immunostaining (Figure 3). Circulating COMP-Ang1 increased as early as 12 hours after treatment, peaked at 1 to 2 weeks, declined gradually thereafter, and returned to control levels at 6 weeks after treatment (Figure 3A). The peak concentrations of circulating COMP-Ang1 were ≈3.5 to 4.5 μg. Significant enlargement of postcapillary venules, capillaries (distinctively, only the venous end of capillaries was enlarged), collecting venules, and terminal arterioles, but not segmental arterioles, was notice-

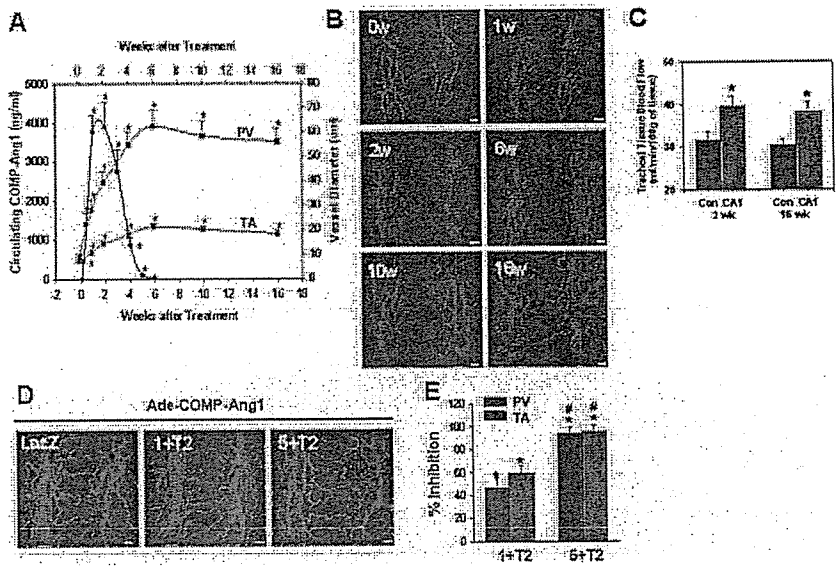

Figure 3. Effect of adenoviral COMP-Ang1 on postcapillary venules and terminal arterioles and blood flow. A through D, FVB/N mice were treated with 1×10^9 pfu Ade-COMP-Ang1 (n=6). At the indicated times, circulating plasma levels of COMP-Ang1 were measured by ELISA (A, black circle), and tracheal vessels were visualized with PECAM-1 immunostaining (B, red). The diameters of postcapillary venules (PV, brown curve) and terminal arterioles (TA, blue curve) are shown. Diameters of 35 to 40 PV/5 fields and 10 to 12 TA/10 fields were measured at the edge of cartilage rings in each mouse. Values are mean±SD from 4 to 5 mice. *$P<0.05$ vs control period. Scale bar=50 μm. C, Laser-Doppler flowmetric analyses for tracheal tissue blood flows of the mice treated with 1×10^9 pfu Ade-LacZ (Con) or 1×10^9 pfu Ade-COMP-Ang1 (CA1). Quantification of tracheal blood flows at 2 and 16 weeks after treatment with Con or CA1. Bars represent mean±SD from 4 to 5 mice. *$P<0.05$ vs Con. D and E, FVB/N mice were pretreated with 1×10^8 (1+T2) or 5×10^8 (5+T2) pfu Ade-sTie2-Fc (n=5 each), or 5×10^8 pfu Ade-LacZ (LacZ, n=5) at 24 hours before 1×10^8 pfu Ade-COMP-Ang1 treatment. Two weeks later, tracheal vessels were visualized by PECAM-1 immunostaining (D, red). Scale bar=50 μm. Diameters of 35 to 40 PV/5 fields and 10 to 12 TA/10 fields were measured at the edge of cartilage rings in each mouse. E, Bars represent the mean±SD from 5 experiments as percentage of inhibition of vascular remodeling induced by the pretreatment. Vascular remodeling induced by pretreatment of the Ade-LacZ is arbitrarily given as 100%. *$P<0.05$ vs LacZ, #$P<0.05$ vs 1+T2.

able at 1 week after the Ade-COMP-Ang1 treatment (Figure 3B). The vascular enlargements induced by Ade-COMP-Ang1 increased further for up to 6 weeks and then reached a plateau (Figure 3A and 3B). For example, the diameter of postcapillary venules increased 4.3-fold at 2 weeks, 6.0-fold at 4 weeks, and 6.8-fold at 6 weeks (Figure 3A). The enlargement of terminal arterioles was also significant beginning at 1 week after the treatment and increased in a time-dependent manner. However, the increase in diameter in terminal arterioles was less than that in postcapillary venules (Figure 3A and 3B). Importantly, the size of Ade-COMP-Ang1–induced enlarged blood vessels did not significantly decrease for as long as 16 weeks after the treatment, although circulating COMP-Ang1 returned to the control level at 6 weeks after treatment (Figure 3A). In comparison, diameters of tracheal vessels in mice treated with Ade-LacZ were indistinguishable between the control and experimental periods (data not shown). Using a laser-Doppler flowmeter, tracheal tissue blood flows were measured at 2 weeks (the peak level of circulating COMP-Ang1) and 16 weeks (undetectable level of circulating COMP-Ang1) after Ade-LacZ or Ade-COMP-Ang1 treatment. At 2 weeks, tracheal tissue blood flow was increased ≈25% in the mice treated with Ade-COMP-Ang1 compared with the mice treated with Ade-LacZ (Figure 3C and 3D). At 16 weeks, importantly, increased tracheal tissue blood flow by Ade-COMP-Ang1 was not significantly changed (Figure 3C and 3D). These results indicate that long term and sustained circulating COMP-Ang1 treatment induces long-lasting enlargement of tracheal blood vessels with long-lasting enhancement of tissue blood flow in the adult mice.

Tie2 Activation Is Involved in COMP-Ang1–Induced Vascular Remodeling

To determine the involvement of Tie2 activation in COMP-Ang1–induced vascular remodeling, the mice were pretreated with 1×10^8 pfu or 5×10^8 pfu Ade-sTie2-Fc at 24 hours before 1×10^8 pfu Ade-COMP-Ang1 treatment. Two weeks later, the diameters of postcapillary venules and terminal arterioles were measured. Pretreatment with 1×10^8 pfu or 5×10^8 pfu Ade-sTie2-Fc suppressed COMP-Ang1–induced vascular remodeling to the following extent: 46.5±7.7% or 93.5±6.4% in postcapillary venules and 59.7±6.6% or 95.1±5.7% in terminal arterioles, respectively (Figure 3E and 3F). These data indicate that COMP-Ang1–induced vascular remodeling is mainly mediated through Tie2 activation in adult tracheal vessels.

Long-Term and Sustained Circulating COMP-Ang1 Induces Various Vascular Remodeling in Different Organ

Both mice treated with Ade-LacZ (1×10^9 pfu) and those treated with Ade-COMP-Ang1 (1×10^9 pfu) appeared generally healthy, as they gained weight normally. However, the skin of mice treated with Ade-COMP-Ang1 appeared strikingly redder than the skin of mice treated with Ade-LacZ, beginning 10 to 14 days after the treatment. The Ade-COMP-

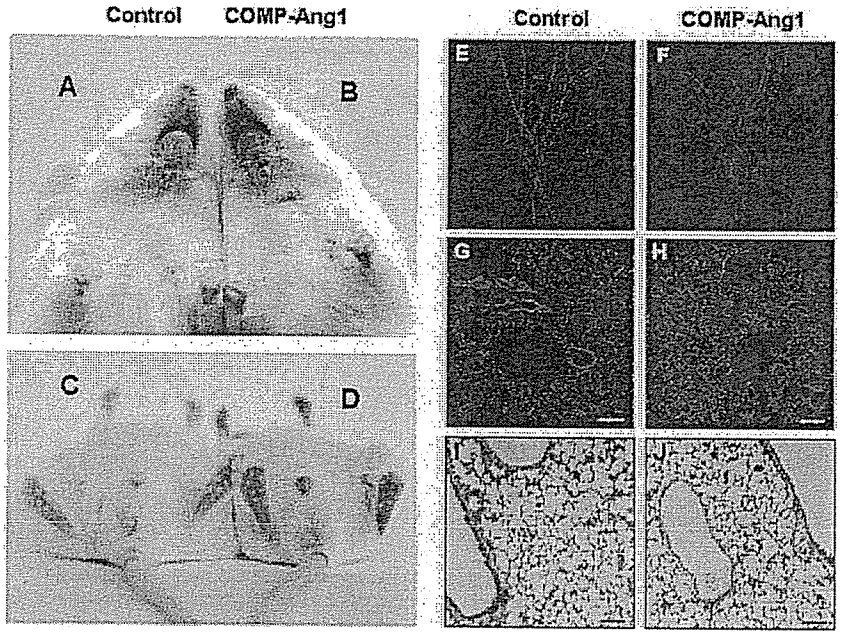

Figure 4. Effect of adenoviral COMP-Ang1 on skin color and vascular remodeling in ear skin and lung at 16 weeks after treatment. FVB/n mice were treated with 1×10^9 pfu Ade-LacZ or Ade-COMP-Ang1. Sixteen weeks later, the skin color of the face, hands, soles, penis, and tail were photographed (A, B, C, and B), blood vessels in ear skin (E and F) and lungs (G and H) were visualized with PECAM-1 (CD31) immunostaining (red), and sections of lungs were stained with H&E (I and J). The mice treated with Ade-COMP-Ang1 show overt skin redness, have prominently enlarged blood vessels in the ear skin, and have more dense PECAM-1–positive endothelial cells in the lung without overt histologic alteration compared with the mice treated with Ade-LacZ. The results from 4 experiments were similar. Scale bar=50 μm.

Ang1–induced skin redness persisted for as long as 16 weeks after the treatment (Figure 4). Sixteen weeks after the treatment, skin color in hair-sparse portions such as the face, hands, soles, penis, and tail of mice treated with Ade-COMP-Ang1 were distinctly redder than those of mice treated with Ade-LacZ. Blood vessels of the ear and capillaries of the heart, adrenal cortex, and liver of the mice treated with Ade-COMP-Ang1 were enlarged (Figures 4 and 5). More PECAM-1–positive endothelial cells were present in the lung, heart, liver, and renal medulla of mice treated with Ade-COMP-Ang1 compared with the mice treated with Ade-LacZ (Figures 4 and 5 and online Figure I in the data supplement). However, blood vessels of the renal cortex, including glomeruli, and intestinal villi of the mice treated with Ade-COMP-Ang1 and the mice treated with Ade-LacZ were indistinguishable. In addition, the body weights, systemic blood pressures, and heart rates of the 2 groups of mice were indistinguishable. These results indicate that long-term and sustained circulating COMP-Ang1 treatment induces long-lasting tissue-specific vascular remodeling in different blood vessels without notable changes in systemic blood pressure and heart rate (online Table I).

Induction of Tie2 Could Be Involved in Permanent Changes of COMP-Ang1–Induced Vascular Remodeling

Based on these observations, we asked whether Tie2 expression was more abundant in postcapillary venules than termi-

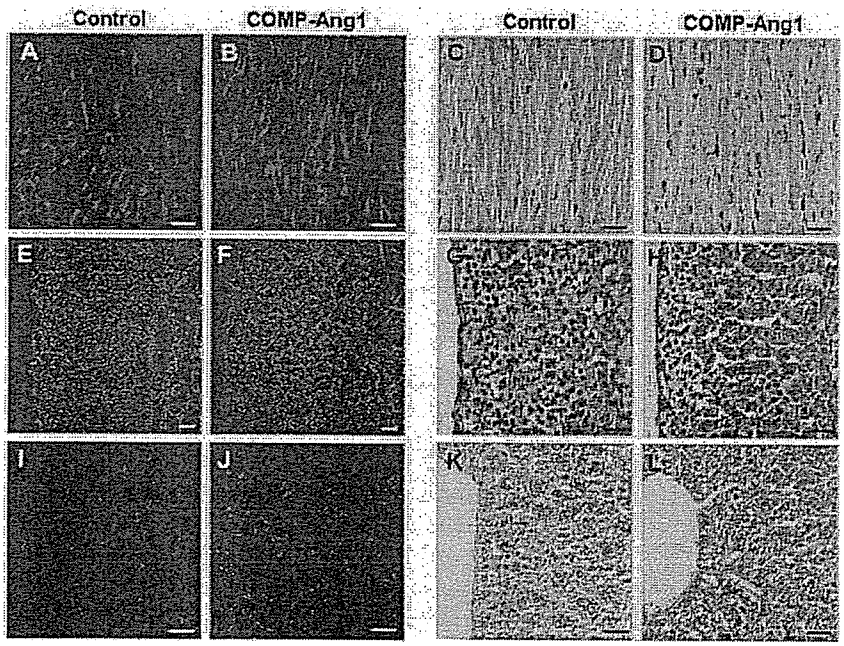

Figure 5. Effect of adenoviral COMP-Ang1 on vascular remodeling in heart, adrenal cortex, and liver at 16 weeks after the treatment. FVB/n mice were treated with 1×10^9 pfu Ade-LacZ or Ade-COMP-Ang1. Sixteen weeks later, blood vessels in heart (A through D), adrenal cortex (E through H), and liver (I through L) were visualized with PECAM-1 (CD31) immunostaining (red), and the sections were stained with H&E. The mice treated with Ade-COMP-Ang1 have enlarged capillaries in the heart and adrenal cortex and more PECAM-1–positive endothelial cells in the liver compared with the mice treated with Ade-LacZ. The results from 4 experiments were similar. Scale bar=25 μm.

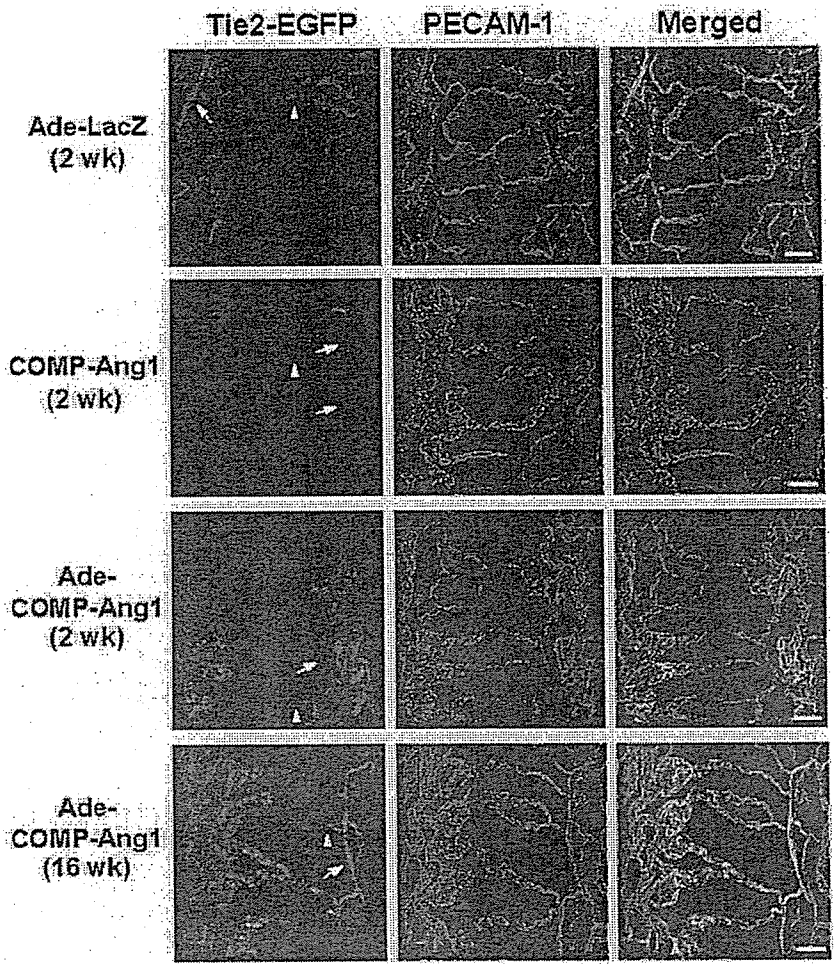

Figure 6. Induction of Tie2 expression in COMP-Ang1–induced vascular remodeling. Tie2-GFP transgenic mice (10 weeks old) were treated with daily injection of 200 μg of COMP-Ang1 recombinant protein (COMP-Ang1) for 2 weeks or a single injection of 1×10^9 pfu Ade-LacZ or Ade-COMP-Ang1. At 2 and 16 weeks after the beginning of the treatments, Tie2 expression in tracheal vessels was visualized by GFP expression (green) and PECAM-1 immunostaining (red), and the images were merged. The results from 4 experiments were similar. Arrowhead indicates terminal arterioles; arrow, precapillary arterioles. Scale bar=50 μm.

nal arterioles in mouse trachea. Therefore, we examined the extent of Tie2 expression using transgenic mice with Tie2 promoter–driven green fluorescent protein (GFP).[12] In the tracheal mucosa of adult mice, Tie2 expression was not detectable in most endothelial cells of postcapillary venules, whereas it was moderately expressed in endothelial cells of terminal and precapillary arterioles of tracheal vessels (Figure 6). Thus, differential enlargement of tracheal vessels on COMP-Ang1 stimulation is not dependent on the extent of Tie2 expression. However, Tie2 expression was markedly increased in endothelial cells of collecting venules, venules, postcapillary venules, and capillaries at 2 weeks after the Ade-COMP-Ang1 treatment (Figure 6), which is somewhat consistent with a recent report with Ade-Ang1.[8] Tie2 expression was further increased in endothelial cells of the same vessels at 16 weeks after the Ade-COMP-Ang1 treatment (Figure 6). In contrast, Tie2 expression was not changed in any endothelial cells of enlarged tracheal vessels at 2 weeks after the recombinant COMP-Ang1 protein treatment (Figure 6). Area densities of Tie2 expression in a given microscopic field area (0.22 mm^2) for arterioles, capillaries, and venules in tracheal mucosa were 8.2±1.7, 2.8±0.4, and 3.3±0.6% (mean±SD from 4 mice), respectively, after Ade-LacZ treatment (at 2 weeks); 7.6±1.9, 3.1±0.5, and 3.7±0.6% after COMP-Ang1 protein treatment (at 2 weeks); 11.3±2.2, 10.3±1.7, and 28.1±5.4% after Ade-COMP treatment (at 2 weeks); and 13.3±2.7, 18.2±3.5, and 47.7±7.2 after Ade-COMP treatment (at 16 weeks). In addition, Tie2 expression was notably higher in the enlarged veins of abdominal skin and the sinusoidal capillaries in liver of the mice treated with Ade-COMP-Ang1 than the mice treated with Ade-LacZ at 16 weeks after the treatment (online Figure II). Thus, Tie2 expression in venular and capillary endothelial cells could be induced with long-term and sustained Tie2 stimulation induced by Ade-COMP-Ang1 but not with short-term spiked Tie2 stimulation induced by recombinant COMP-Ang1 protein.

COMP-Ang1–Induced Vascular Enlargement Could Result From Circumferential Endothelial Cell Proliferation

COMP-Ang1–induced enlargement of blood venules appears to result from endothelial cell proliferation rather than vasodilation or endothelial cell hypertrophy because the endothelial cells were normal in size (Figure 7A and 7B). To test this possibility, we examined by immunostaining the number of endothelial cells positive for phosphohistone H3 (nuclear protein of diving cell). Numerous phosphohistone H3–positive immunostained endothelial cells were detected in various portions including postcapillary venules, capillaries, collect-

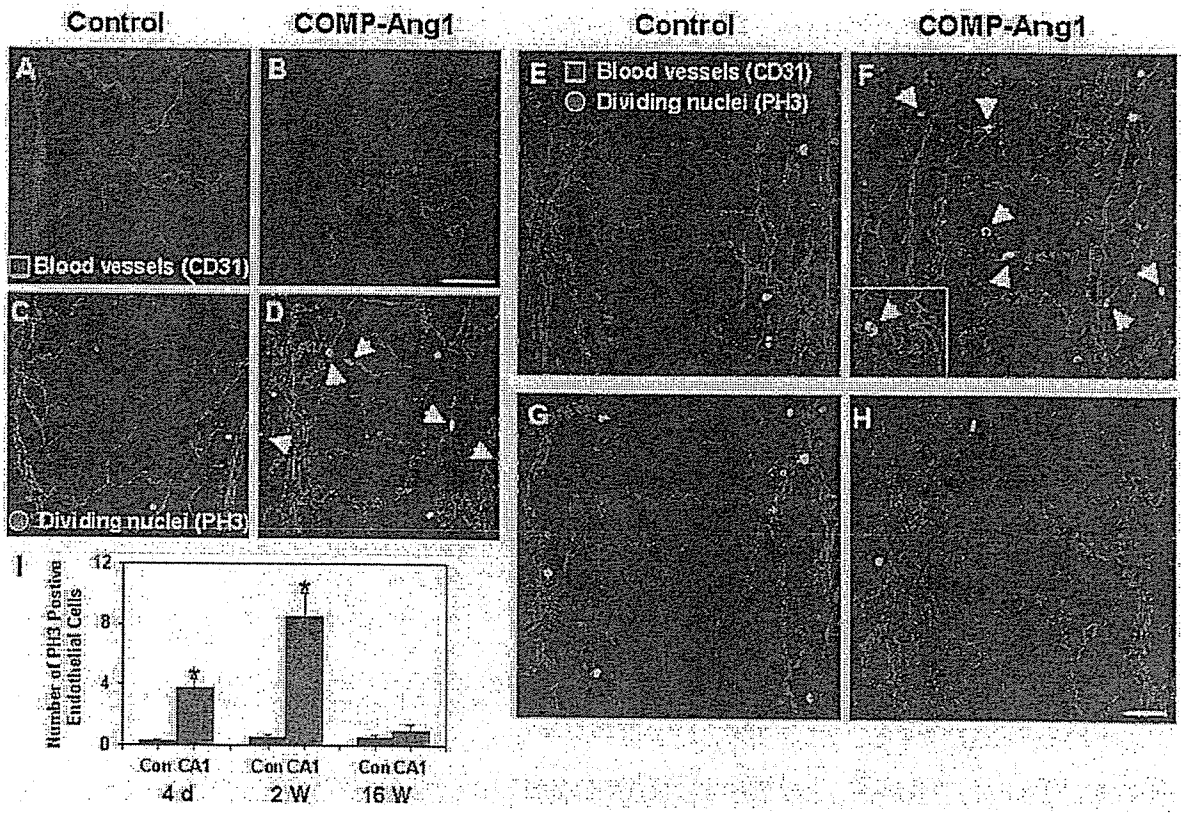

Figure 7. Increased number of dividing endothelial cells during COMP-Ang1–induced enlargement. FVB/N mice were treated with 1×10^9 pfu Ade-LacZ (control; A, C, E, and G) or Ade-COMP-Ang1 (COMP-Ang1; B, D, F, and H). Four days (C and D), 2 weeks (E and F), and 16 weeks (G and H) later, tracheal vessels were visualized with PECAM-1 (CD31) immunostaining (red) and phosphohistone H3 (PH3) immunostaining (green). F, Arrow indicates PH3-immunopositive endothelial cells; white square, PH3-immunopositive endothelial cells in postcapillary venule at higher magnification. Scale bar=50 μm. I, Number of PH3-immunopositive endothelial cells in a given 0.21 mm^2 area. Bars represent mean±SD from 4 mice. Con indicates control; CA1, COMP-Ang1. *$P<0.05$ vs Con.

ing venules, venules, and terminal arterioles of tracheal vessels at 4 days and 2 weeks after the Ade-COMP-Ang1 treatment (Figure 7D, 7F, and 7I) or after recombinant COMP-Ang1 protein treatment (data not shown). However, almost no phosphohistone H3–positive endothelial cells were detected in any portion of tracheal vessels at 4 days or 2 and 16 weeks after the Ade-LacZ treatment and at 16 weeks after the Ade-COMP-Ang1 treatment (Figure 7C, 7E, 7G, and 7I). These findings indicate that vascular enlargement induced by COMP-Ang1 is more likely to result from endothelial cell proliferation depending on concentration of circulating COMP-Ang1 than from vasodilation or endothelial cell hypertrophy.

COMP-Ang1–Induced Postcapillary Venule Enlargement Is Not Accompanied by Pericyte Recruitment

Ang1 is known to be a strong growth factor for pericyte recruitment to nascent endothelial cells during vasculogenesis in physiological and pathological conditions.[3–5] Therefore, we examined the interaction between endothelial cells and pericytes in the enlarged blood vessels of the trachea by double-immunostaining for endothelial cells and pericytes at 4 weeks after Ade-LacZ or Ade-COMP-Ang1 treatment. The interaction of endothelial cells and pericytes in most of tracheal blood vessels (except postcapillary venules) in mice that received Ade-COMP-Ang1 was similar to that in mice that received Ade-LacZ (Figure 8). Although less interaction of endothelial cells with pericytes was found on the enlarged postcapillary venules than elsewhere, the number of pericytes of the enlarged postcapillary venules was similar to the control postcapillary venules (Figure 8). Thus, COMP-Ang1 did not promote pericyte recruitment to the COMP-Ang1–induced enlarged venules in the trachea.

Discussion

The most important and novel finding in this study is that enlargement of tracheal blood vessels and enhancement of tracheal tissue blood flow induced by long-term and sustained exposure to COMP-Ang1 had not regressed for up to 16 weeks, despite the fact that exposure to COMP-Ang1 had already been discontinued at 6 to 7 weeks in adult mice. In comparison, enlargement of tracheal blood vessels induced by short-term intermittent exposure to COMP-Ang1 regressed on discontinuation of recombinant COMP-Ang1 treatment. Therefore, long-lasting vascular enlargement and enhancement of blood flow can be achieved by long-term and sustained exposure to COMP-Ang1.

Like other therapeutic proteins, circulating COMP-Ang1 rapidly disappeared in the plasma, probably because of its trapping by the Tie2 receptor of lung endothelial cells.[15]

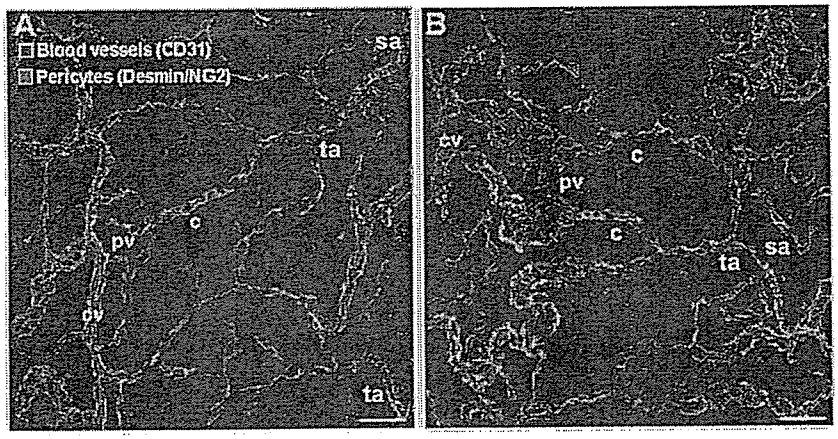

Figure 8. Interaction between endothelial cells and pericytes in COMP-Ang1–induced enlarged tracheal vessels. FVB/n mice were treated with 1×10^9 pfu Ade-COMP-Ang1 (B) or Ade-LacZ (A). Four weeks later, tracheal vessels were visualized with PECAM-1 (CD31) immunostaining (red), and pericytes were visualized with desmin/NG2 immunostaining (green). The results from 4 experiments were similar. Scale bar=50 μm.

However, we were able to achieve long-term (>4 weeks) and sustained (>1000 ng/mL) circulating COMP-Ang1 in mice by a single intravenous injection of 1×10^9 pfu Ade-COMP-Ang1. Throughout these experiments, we learned that long-term (≈6 weeks) and sustained exposure to COMP-Ang1 produced long-lasting enlargement of postcapillary venules and terminal arterioles in the tracheal mucosa, whereas short-term (≈2 weeks) and intermittent exposure to COMP-Ang1 produced reversible enlargements of these vessels. Similar to our results, another study found that long-term (4 weeks) sustained exposure to vascular endothelial growth factor (VEGF) produced long-lasting acquired vascular remodeling in liver, whereas short-term (2 weeks) sustained exposure to VEGF produced reversible vascular remodeling.[16] What are the major mechanisms and factors that produce long-lasting and reversible vascular remodeling? Is there a threshold stimulation of Tie2 by COMP-Ang1 that can produce permanent enlargement? Our results suggest that auto-amplification of Tie2 expression by treatment with COMP-Ang1 above a certain dose and exposure period could be one of the mechanisms. Once Tie2 expression is activated by a long-term and excess exposure to COMP-Ang1, after discontinuation of COMP-Ang1, the subsequent activation of Tie2 might be achieved by endogenous circulating Ang1 or increased shear stress caused by increased blood flow.[17] However, auto-amplification of Tie2 expression cannot be achieved below a certain dose and exposure period of COMP-Ang1, as evidenced by the experiments with intravenous administration of COMP-Ang1 recombinant protein. Therefore, the dose and the exposure period of COMP-Ang1 or VEGF should be considered in any therapeutic approaches where permanent vascular enlargements are needed to alleviate dysfunctions of ischemic tissues.

Tie1, an endothelial-specific receptor tyrosine kinase, shares a high degree of homology with Tie2. Although Tie1 was isolated more than a decade ago,[18] no ligand had been found to activate it. Recently, Saharinen et al demonstrated that COMP-Ang1 stimulated Tie1 phosphorylation in cultured endothelial cells.[19] Moreover, they showed that COMP-Ang1–induced Tie1 activation was amplified via Tie2 and was more efficient than native Ang1- and Ang4-induced Tie1 activation. Thus, COMP-Ang1 and Ang1 are now known to be activating ligands for both Tie1 and Tie2. However, our data indicate that COMP-Ang1–induced vascular remodeling in adult tracheal vessels is mainly mediated through activation of Tie2, not by Tie1. (See expanded Discussion section in the online data supplement.)

Although Ang1 induces vascular enlargement and has therapeutic benefits to ischemic tissues in several experimental animal models,[6,7,9] little is known about whether the vascular enlargement is accompanied by enhanced blood flow. Our results showed that COMP-Ang1–induced vascular enlargement was accompanied by enhanced tissue blood flow in the trachea. Therefore, enhanced blood flow through arteriolar and venular enlargements induced by COMP-Ang1 could provide a great therapeutic benefit to ischemic peripheral tissues. In fact, Ang1-induced vessel enlargement is a unique characteristic among many growth factors. Our immunohistological examination of phosphohistone H3 revealed that COMP-Ang1–induced vascular enlargements were evidently the result of endothelial proliferation, which is consistent with a recent report.[14] Thus, arteriolar and venular enlargements are achieved mainly by circumferential endothelial proliferation, which is a unique phenomenon and is different from multidirectional endothelial cell proliferation during vasculogenesis and angiogenesis. Moreover, our results revealed that different organs showed different sensitivities to long-term and sustained COMP-Ang1. In fact, blood vessels in the skin, heart, adrenal cortex, and liver, among other organs, are relatively sensitive to the COMP-Ang1–induced vascular enlargement. Therefore, COMP-Ang1 could provide a great therapeutic benefit to patients with delayed skin wound healing and ischemic heart diseases through its ability to promote vascular remodeling. Nevertheless, the mice treated with long-lasting and sustained COMP-Ang1 did not show any significant changes in body weight, systemic blood pressure, or heart rate. More detailed analysis will be necessary to clarify how it is possible that the mice with enlarged blood vessels caused by long-term and sustained COMP-Ang1 have normal blood pressure and heart rate.

Ang1 is known to be a strong growth factor for pericyte recruitment to nascent endothelial cells during development.[3–5] This Ang1-induced pericyte recruitment is related to the Ang1-induced antileakage effect on VEGF and proinflammatory stimuli.[5] However, our results show a lower number and poorer covering of pericytes in COMP-Ang1–

induced enlarged postcapillary venules. In fact, in a mouse model that completely blocks pericyte recruitment to developing vessels by injection of antagonistic monoclonal antibody against platelet-derived growth factor receptor-β, Angl is able to restore a hierarchical architecture of growing blood vessels and rescues retinal edema and hemorrhage even in the absence of pericyte recruitment.[20] Thus, COMP-Angl may be able to assemble endothelial cells in a frame of hierarchical architecture without pericyte recruitment in the COMP-Angl–induced enlarged blood vessels.

In conclusion, long-lasting vascular enlargement and enhancement of blood flow can be achieved by long-term and sustained exposure to COMP-Angl.

Acknowledgments

Supported, in part, by the Bio-Challenge Program and the National Research Laboratory Program (2004-02376 to G.Y.K.) of the Korean Ministry of Science and Technology, the Korea Health R&D Project (0405-DB01-0104-0006 to G.Y.K.), the Ministry of Health & Welfare, and the Korea Science and Engineering Foundation (R01-2004-000-10045-0 to B.H.J.). Also supported by National Institutes of Health grants HL-24136 and HL-59157 from the National Heart, Lung and Blood Institute (to D.M.D.).

References

1. Davis S, Aldrich TH, Jones PF, Acheson A, Compton DL, Jain V, Ryan TE, Bruno J, Radziejewski C, Maisonpierre PC, Yancopoulos GD. Isolation of angiopoietin-1, a ligand for the TIE2 receptor by secretion-trap expression cloning. *Cell.* 1996;87:1161–1169.
2. Dumont DJ, Gradwohl G, Fong GH, Puri MC, Gertsenstein M, Auerbach A, Breitman ML. Dominant-negative and targeted null mutations in the endothelial receptor tyrosine kinase, tek, reveal a critical role in vasculogenesis of the embryo. *Genes Dev.* 1994;8:1897–1909.
3. Suri C, Jones PF, Patan S, Bartunkova S, Maisonpierre PC, Davis S, Sato TN, Yancopoulos GD. Requisite role of angiopoietin-1, a ligand for the TIE2 receptor, during embryonic angiogenesis. *Cell.* 1996;87:1171–1180.
4. Suri C, McClain J, Thurston G, McDonald DM, Zhou H, Oldmixon EH, Sato TN, Yancopoulos GD. Increased vascularization in mice overexpressing angiopoietin-1. *Science.* 1998;282:468–471.
5. Thurston G, Suri C, Smith K, McClain J, Sato TN, Yancopoulos GD, McDonald DM. Leakage-resistant blood vessels in mice transgenically overexpressing angiopoietin-1. *Science.* 1999;286:2511–2514.
6. Shyu KG, Manor O, Magner M, Yancopoulos GD, Isner JM. Direct intramuscular injection of plasmid DNA encoding angiopoietin-1 but not angiopoietin-2 augments revascularization in the rabbit ischemic hindlimb. *Circulation.* 1998;98:2081–2087.
7. Chae JK, Kim J, Lim ST, Chung MJ, Kim WH, Kim HG, Ko JK, Koh GY. Co-administration of angiopoietin-1 and vascular endothelial growth factor enhances collateral vascularization. *Arterioscler Thromb Vasc Biol.* 2000;20:2573–2578.
8. Baffert F, Thurston G, Rochon-Duck M, Le T, Brekken R, McDonald DM. Age-related changes in vascular endothelial growth factor dependency and angiopoietin-1-induced plasticity of adult blood vessels. *Circ Res.* 2004;94:984–992.
9. Zhou YF, Stabile E, Walker J, Shou M, Baffour R, Yu Z, Rott D, Yancopoulos GD, Rudge JS, Epstein SE. Effects of gene delivery on collateral development in chronic hypoperfusion: diverse effects of angiopoietin-1 versus vascular endothelial growth factor. *J Am Coll Cardiol.* 2004;44:897–903.
10. Cho CH, Kammerer RA, Lee HJ, Steinmetz MO, Ryu YS, Lee SH, Yasunaga K, Kim KT, Kim I, Choi HH, Kim W, Kim SH, Park SK, Lee GH, Koh GY. COMP-Angl: a designed angiopoietin-1 variant with nonleaky angiogenic activity. *Proc Natl Acad Sci USA.* 2004;101:5547–5552.
11. Hwang SJ, Choi HH, Kim KT, Hong HJ, Koh GY, Lee GM. Expression and purification of recombinant human angiopoietin-2 produced in CHO cells. *Protein Express Purif.* 2005;39:175–183.
12. Schlaeger TM, Bartunkova S, Lawitts JA, Teichmann G, Risau W, Deutsch U, Sato TN. Uniform vascular-endothelial-cell-specific gene expression in both embryonic and adult transgenic mice. *Proc Natl Acad Sci USA.* 1997;94:3058–3063.
13. Baluk P, Raymond WW, Ator E, Coussens LM, McDonald DM, Caughey GH. Matrix metalloproteinase-2 and -9 expression increases in Mycoplasma-infected airways but is not required for microvascular remodeling. *Am J Physiol Lung Cell Mol Physiol.* 2004;287:L307–L317.
14. McDonald DM. Endothelial gaps and permeability of venules in rat tracheas exposed to inflammatory stimuli. *Am J Physiol.* 1994;266:L61–L83.
15. Cho CH, Kammerer RA, Lee HJ, Yasunaga K, Kim KT, Choi HH, Kim W, Kim SH, Park SK, Lee GM. A designed angiopoietin-1 variant, COMP-Angl, protects against radiation-induced endothelial cell apoptosis. *Proc Natl Acad Sci USA.* 2004;101:5553–5558.
16. Dor Y, Djonov V, Abramovitch R, Itin A, Fishman GI, Carmeliet P, Goelman G, Keshet E. Conditional switching of VEGF provides new insights into adult neovascularization and pro-angiogenic therapy. *EMBO J.* 2002;21:1939–1947.
17. Lee HJ, Koh GY. Shear stress activates Tie2 receptor tyrosine kinase in human endothelial cells. *Biochem Biophys Res Commun.* 2003;304:399–404.
18. Partanen J, Armstrong E, Makela TP, Korhonen J, Sandberg M, Renkonen R, Knuutila S, Huebner K, Alitalo K. A novel endothelial cell surface receptor tyrosine kinase with extracellular epidermal growth factor homology domains. *Mol Cell Biol.* 1992;12:1698–1707.
19. Saharinen P, Kerkela K, Ekman N, Marron M, Brindle N, Lee GM, Augustin H, Koh GY, Alitalo K. Multiple angiopoietin recombinant proteins activate the Tie1 receptor tyrosine kinase and promote its interaction with Tie2. *J Cell Biol.* 2005;169:239–243.
20. Uemura A, Ogawa M, Hirashima M, Fujiwara T, Koyama S, Takagi H, Honda Y, Wiegand SJ, Yancopoulos GD, Nishikawa S. Recombinant angiopoietin-1 restores higher-order architecture of growing blood vessels in mice in the absence of mural cells. *J Clin Invest.* 2002;110:1619–1628.

Am J Physiol Heart Circ Physiol 288: H1444–H1450, 2005.
First published November 11, 2004; doi:10.1152/ajpheart.00266.2004.

Adrenomedullin enhances therapeutic potency of bone marrow transplantation for myocardial infarction in rats

Takafumi Fujii,[1] Noritoshi Nagaya,[2,3] Takashi Iwase,[2] Shinsuke Murakami,[2] Yoshinori Miyahara,[1] Kazuhiro Nishigami,[3] Hatsue Ishibashi-Ueda,[5] Mikiyasu Shirai,[1] Takefumi Itoh,[2] Kozo Ishino,[6] Shunji Sano,[6] Kenji Kangawa,[4] and Hidezo Mori[1]

Departments of [1]Cardiac Physiology, [2]Regenerative Medicine and Tissue Engineering, [3]Internal Medicine, [4]Biochemistry, and [5]Pathology, National Cardiovascular Center, Osaka; and [6]Department of Cardiovascular Surgery, Okayama University Medical School, Okayama, Japan

Submitted 18 March 2004; accepted in final form 19 October 2004

Fujii, Takafumi, Noritoshi Nagaya, Takashi Iwase, Shinsuke Murakami, Yoshinori Miyahara, Kazuhiro Nishigami, Hatsue Ishibashi-Ueda, Mikiyasu Shirai, Takefumi Itoh, Kozo Ishino, Shunji Sano, Kenji Kangawa, and Hidezo Mori. Adrenomedullin enhances therapeutic potency of bone marrow transplantation for myocardial infarction in rats. *Am J Physiol Heart Circ Physiol* 288: H1444–H1450, 2005. First published November 11, 2004; doi: 10.1152/ajpheart.00266.2004.—Adrenomedullin (AM), a potent vasodilator, induces angiogenesis and inhibits cell apoptosis through the phosphatidylinositol 3-kinase/Akt pathway. Transplantation of bone marrow-derived mononuclear cells (MNC) induces angiogenesis. We investigated whether infusion of AM enhances the therapeutic potency of MNC transplantation in a rat model of myocardial infarction. Immediately after coronary ligation, bone marrow-derived MNC (5×10^6 cells) were injected into the ischemic myocardium, followed by subcutaneous administration of 0.05 $\mu g \cdot kg^{-1} \cdot min^{-1}$ AM (AM-MNC group) or saline (MNC group) for 3 days. Another two groups of rats received subcutaneous administration of AM alone (AM group) or saline (control group). Hemodynamic and histological analyses were performed 4 wk after treatment. Cardiac infarct size was significantly smaller in the MNC and AM groups than in the control group. A combination of AM infusion and MNC transplantation demonstrated a further decrease in infarct size. Left ventricular (LV) maximum change in pressure over time and LV fractional shortening were significantly improved only in the AM-MNC group. AM significantly increased capillary density in ischemic myocardium, suggesting the angiogenic potency of AM. AM infusion plus MNC transplantation demonstrated a further increase in capillary density compared with AM or MNC alone. Although MNC apoptosis was frequently observed 72 h after transplantation, AM markedly decreased the number of terminal deoxynucleotidyl transferase-mediated dUTP nick-end labeling-positive cells among the transplanted MNC. In conclusion, AM enhanced the angiogenic potency of MNC transplantation and improved cardiac function in rats with myocardial infarction. This beneficial effect may be mediated partly by the angiogenic property of AM itself and by its antiapoptotic effect on MNC.

angiogenesis; apoptosis; mononuclear cell

DESPITE THE RECENT REMARKABLE progress in medical and surgical treatment for ischemic heart disease, this disease remains a major cause of death worldwide (5). Bone marrow-derived mononuclear cells (MNC) contain various kinds of cell lineages and numerous cytokines that contribute to neovascularization (1, 15). In fact, autologous transplantation of bone marrow cells has been shown to enhance angiogenesis and improve cardiac function in an animal model of cardiac ischemia (6, 9, 10). Recent human studies have demonstrated beneficial effects of transplanted MNC in patients with ischemic heart disease (23, 25). However, some patients fail to respond to this cell therapy. Thus a novel therapeutic strategy to enhance the angiogenic property of MNC is desirable.

Adrenomedullin (AM) is a potent vasodilator peptide that was originally isolated from human pheochromocytoma (8). We have shown that infusion of AM has beneficial hemodynamic and renal effects in patients with heart failure (17). On the other hand, AM has been shown to activate the phosphatidylinositol 3-kinase (PI3-kinase)/Akt-dependent pathway in vascular endothelial cells, which is considered to regulate multiple critical steps in angiogenesis including endothelial cell proliferation, migration, and capillary-like formation (14, 22). In fact, we have shown that AM gene transfer induces therapeutic angiogenesis in a rabbit model of hindlimb ischemia via activation of Akt (24). These findings suggest that AM may play an important role in the regulation of vascular regeneration. In addition, AM has been shown to exert an antiapoptotic effect on a variety of cells including vascular endothelial cells (7, 20). Taking these findings together, combination therapy with MNC transplantation and AM infusion may have additional or synergetic effects on therapeutic angiogenesis for the treatment of ischemic heart disease.

Thus the purposes of this study were *1*) to investigate whether infusion of AM enhances the angiogenic potency of MNC transplantation in a rat model of myocardial infarction, and *2*) to investigate the effects of AM on survival and differentiation of the transplanted MNC to examine the underlying mechanisms of the effects induced by AM.

MATERIALS AND METHODS

Animal model. Myocardial infarction was produced in male Lewis rats weighing 200–220 g by left coronary ligation. In brief, after rats were anesthetized by intraperitoneal injection of pentobarbital sodium (30 mg/kg body wt), they were ventilated artificially. The heart was exposed via left thoracotomy, and the left coronary artery was ligated 2–3 mm from its origin between the pulmonary artery conus and the left atrium using a 6-0 proline suture. Finally, the heart was restored to its normal position, and the chest was closed. The Animal Care Committee of the National Cardiovascular Center approved this experimental protocol.

Address for reprint requests and other correspondence: N. Nagaya, Dept. of Regenerative Medicine and Tissue Engineering, National Cardiovascular Center Research Institute, 5-7-1 Fujishirodai, Suita, Osaka 565-8565, Japan (E-mail: nnagaya@ri.ncvc.go.jp).

The costs of publication of this article were defrayed in part by the payment of page charges. The article must therefore be hereby marked "*advertisement*" in accordance with 18 U.S.C. Section 1734 solely to indicate this fact.

Preparation of MNC. After Lewis rats were killed, bone marrow from the femur and tibia was collected and put in PBS. Marrow cells were loaded on a 1.077 gradient of Ficoll (Lymphoprep; Nycomed Pharma, Oslo, Norway) and centrifuged at 1,500 rpm for 20 min. The cells were then washed with 10 ml PBS to remove the Ficoll and centrifuged at 2,000 rpm for 10 min. The cells were finally suspended in PBS at a concentration of 5×10^6 cells in 50 μl PBS for transplantation. Fluorescence-activated cell sorting analysis demonstrated that 22 ± 1% of MNC were positive for lectin from ulex europaeus (UEA)-1 lectin (Sigma, St. Louis, MO).

MNC transplantation and AM infusion. Transplantation of bone marrow-derived MNC and/or 3-day infusion of AM was performed immediately after coronary ligation. MNC (5×10^6 cells in 50 μl PBS) were injected into the myocardium at five points in the border zone surrounding the infarct by using a 27-gauge needle. Recombinant human AM (0.05 $\mu g \cdot kg^{-1} \cdot min^{-1}$) was subcutaneously administered by using an osmotic minipump (model 2004; Alza, Palo Alto, CA) for 3 days. The pump was positioned in a pocket constructed in the subcutaneous tissue just below the subscapular region. For control, 5% glucose was infused in a similar manner in the rats receiving coronary ligation. This protocol resulted in the creation of four groups: *1*) AM infusion plus MNC transplantation (AM-MNC group, $n = 15$), *2*) vehicle infusion plus MNC transplantation (MNC group, $n = 14$), *3*) AM infusion plus PBS injection (AM group, $n = 14$), and *4*) vehicle infusion plus PBS injection (control group, $n = 13$).

Echocardiographic studies. Echocardiographic studies were performed 4 wk after surgery using a 7.5-MHz phased-array transducer (model HP SONOS 5500; Hewlett-Packard, Andover, MA). Rats were anesthetized by intraperitoneal injection of pentobarbital sodium (30 mg/kg body wt) as a supplement to maintain mild anesthesia. M-mode tracings were obtained at the level of the papillary muscles. Anterior and posterior end-diastolic wall thickness, left ventricular (LV) end-diastolic and end-systolic dimension, and LV fractional shortening were measured from three consecutive cardiac cycles by the American Society for Echocardiology leading-edge method (21).

Cardiac catheterization. Cardiac catheterization was performed 4 wk after surgery. Rats were anesthetized with intraperitoneal pentobarbital and placed on a heating pad to maintain body temperature at 37–38°C throughout the study. A 1.5 Fr micronanometer-tipped catheter was inserted in the right carotid artery for measurement of heart rate and mean arterial pressure. The catheter was then advanced into the LV for measurement of LV end-diastolic pressure and then replaced with a thermomicroprobe for measurements of cardiac output. These hemodynamic variables were measured with a pressure transducer (UFI, Morro Bay, CA) connected to a polygraph and recorded with a thermal recorder (model 7758 B system; Hewlett-Packard).

Infarct size measurement. After completion of hemodynamic measurements, the heart was arrested by an injection of 2 mmol KCl through the carotid artery, and the cardiac ventricles were excised. The size of myocardial infarction was determined by a previously described method (2). In brief, incisions were made in the LV so that the tissue could be pressed flat. The circumference of the entire flat LV and the visualized infarcted area, as judged from both the epicardial and endocardial sides, was outlined on a clear plastic sheet. The difference in weight between the two marked areas on the sheet was used to determine infarction size and was expressed as a percentage of LV surface area.

Histological analysis of microvessel density. LV myocardium was fixed in 10% formalin. Three cross sections of the LV, cut from apex to base, were obtained from individual rats for comparison among four groups ($n = 5$ each). They were embedded in paraffin and stained with Masson's trichrome for measurement of interstitial fibrosis. In other rats ($n = 5$ each), LV myocardium was embedded in optimum cutting temperature (OCT) compound (Sakura Finetechnical, Tokyo, Japan), snap frozen in liquid nitrogen, and cut into 5-μm-thick sections. Tissue sections were stained for alkaline phosphatase with an indoxyltetrazolium method to detect capillary endothelial cells ($n = 5$ in each group). The number of capillary vessels was counted in the peri-infarct area (a 1.0-mm band next to the scar) excluding scar region using a light microscope at a magnification of ×200. The numbers in five high-power fields in each rat were averaged and expressed as the number of capillary vessels. These morphometric studies were performed by two examiners who were blinded to treatment.

Detection of MNC apoptosis. To examine the antiapoptotic effect of AM on transplanted MNC, red fluorescence-labeled MNC were transplanted into ischemic myocardium in rats with ($n = 5$) and without ($n = 5$) AM infusion. Before implantation into the ischemic heart, suspended MNC were labeled with fluorescent dyes with a PKH26 (Red Fluorescent Cell Linker Kit; Sigma), as reported previously (13). AM was subcutaneously administered by using a minipump for 3 days. Rats were killed 72 h after MNC transplantation. The LV was enucleated, and muscle samples were embedded in OCT compound and snap frozen in liquid nitrogen for the detection of apoptosis. Serial sections of the heart were stained by terminal deoxynucleotidyl transferase-mediated dUTP nick-end labeling (TUNEL) for apoptosis using an in situ apoptosis detection kit (model S7111 Apoptag Fluorescein Kit; Intergen). Apoptosis of transplanted MNC was also evaluated by the detection of cleaved caspase-3-positive cells. In brief, the frozen tissue sections were incubated with anticleaved caspase-3 antibody (Cell Signaling), followed by incubation with FITC-conjugated IgG antibody (BD Pharmingen, San Diego, CA). The number of TUNEL/PKH26 double-positive cells and caspase-3/PKH26 double-positive cells was counted in 10 fields of each rat using a confocal microscopy (Fluoview model 500; Olympus, Tokyo, Japan).

The antiapoptotic effect of AM on MNC was also evaluated by in vitro TUNEL assay. MNC were plated on 12-well plates (1×10^6 cells per well) and cultured in serum-free medium for 24 h with control buffer, AM (1×10^{-7} M), or AM plus wortmannin, a PI3-kinase inhibitor (50 nM). Randomly selected microscopic fields ($n = 10$) were evaluated for calculating the ratio of TUNEL-positive cells to total cells.

Monitoring of implanted MNC in ischemic heart. Additional rats were used to examine whether transplanted MNC differentiate into endothelial cells, cardiomyocytes, vascular smooth muscle cells, or macrophages in the ischemic heart. PKH26 (red fluorescence)-labeled MNC were injected into the ischemic heart in rats with ($n = 8$) and without ($n = 8$) AM infusion. These subgroups of rats were killed 4 wk after coronary ligation. To identify vascular endothelial cells in vivo, FITC-labeled UEA-1 lectin was intravenously administered 30 min before the rats were killed ($n = 5$ in each group). The LV was enucleated, and muscle samples were then embedded in OCT compound, snap frozen in liquid nitrogen, and cut into sections. Sections were counterstained with 4′,6′-diamidino-2-phenylindole (DAPI) to detect nuclei. The number of DAPI/PKH26 double-positive cells and lectin-positive cells in the peri-infarct area was counted in 10 fields of each rat using a confocal microscopy. Frozen sections from other rats ($n = 3$ in each group) were incubated with mouse anticardiac troponin T (Novocastra, Newcastle, UK), anti-α-smooth muscle actin antibody (Dako, Copenhagen, Denmark), and anti-ED1 antibody (Serotec, Oxford, UK), followed by incubation with FITC-conjugated IgG antibody. In other rats (MNC group, $n = 5$; AM-MNC group, $n = 5$), the cardiac muscle from base to apex was transversely cut into 6-μm slices to calculate the number of transplanted MNC present within the heart 4 wk after transplantation. These morphometric studies were performed by two examiners who were blinded to treatment.

Statistical analysis. Numerical values were expressed as means ± SE. Comparisons of parameters among the four groups were performed by one-way ANOVA, followed by Newman-Keuls test for unpaired data. Comparisons of parameters between two groups were made by unpaired Student's *t*-test. A value of $P < 0.05$ was considered significant.

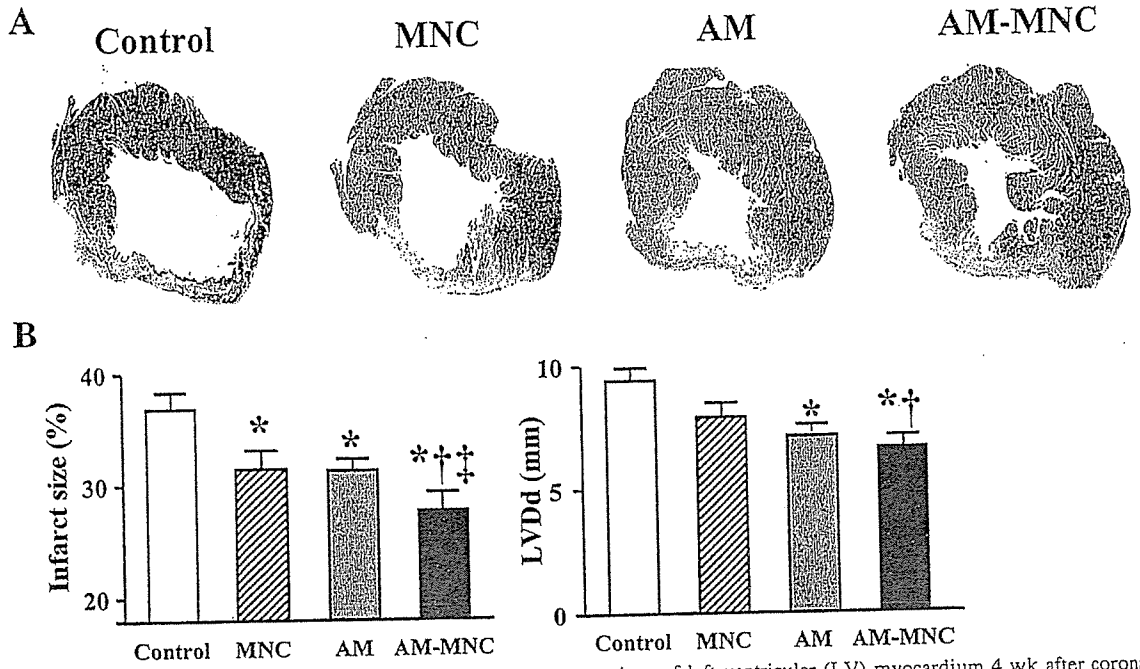

Fig. 1. *A*: representative examples of Masson trichrome-staining of transverse sections of left ventricular (LV) myocardium 4 wk after coronary ligation. *B*: quantitative analysis of infarct size and LV chamber size. Infarcted area and LV end-diastolic diameter (LVDd) of the adrenomedullin-mononuclear cell (AM-MNC) group were significantly smaller than those of the other groups. Values are means ± SE. $*P < 0.05$ vs. control; $\dagger P < 0.05$ vs. MNC; $\ddagger P < 0.05$ vs. AM.

RESULTS

Infarct size and ventricular weight. Moderate-to-large infarcts were observed in the control group after coronary ligation (Fig. 1). However, infarct size was smaller in the MNC, AM, and AM-MNC groups than in the control group. In particular, it was very small in the AM-MNC group. Quantitative analysis also demonstrated that cardiac infarct size in the AM-MNC group was smallest among the four groups. Right ventricular weight was significantly lower in the AM and AM-MNC groups than that in the control group (Table 1). LV weight did not significantly differ among the four groups.

Echocardiographic findings. LV diastolic dimension was smallest in the AM-MNC group, followed by the AM, MNC, and control groups (Fig. 1). LV fractional shortening in the AM-MNC group was also higher than that in the control, MNC, and AM groups (Table 2). Diastolic thickness of the anterior wall was significantly attenuated in the MNC, AM, and AM-MNC groups compared with the control group.

Hemodynamics. Cardiac output in the AM-MNC group was significantly higher than that in the control, MNC, and AM groups (Fig. 2). LV end-diastolic pressure in the MNC, AM, and AM-MNC groups was significantly lower than that in the control group. LV maximum change in pressure over time (dP/d*t*) in the MNC and AM-MNC group were significantly higher than that in the control group. Similarly, LV minimum dP/d*t* was significantly decreased only in the AM-MNC group.

Capillary density. Alkaline phosphatase staining of ischemic myocardium showed marked augmentation of neovascularization in the MNC, AM, and AM-MNC groups compared with the control group (Fig. 3*A*). Quantitative analysis demonstrated that capillary density was significantly higher in the AM-MNC group than in the MNC and AM groups (Fig. 3*B*). Cartilage, bone, or fat was not observed in the transplanted area. No tumor-like cells were seen.

Antiapoptotic effect of AM on MNC. Red fluorescence-labeled MNC were detected in each recipient heart 72 h after transplantation (Fig. 4). TUNEL-positive cells were frequently observed in the MNC group. In contrast, these apoptotic cells

Table 1. *Physiological profiles of four experimental groups*

	Control	MNC	AM	AM-MNC
Number	13	14	14	15
Body weight, g	274±3	285±5	287±3	305±4*
Heart rate, bpm	410±24	404±30	398±33	387±36
MAP, mmHg	101±11	104±13	103±9	116±14*
LV wt/body wt, g/kg	2.4±0.2	2.5±0.2	2.6±0.1	2.5±0.2
RV wt/body wt, g/kg	1.1±0.1	0.9±0.1	0.8±0.1*	0.7±0.1*

Values are means ± SE; number is number of rats in each group. Control group, myocardial infarction rats given vehicle; MNC group, those given mononuclear cells; AM, those given adrenomedullin; AM-MNC, those given AM and MNC; MAP, mean arterial pressure; LV, left ventricle; RV, right ventricle. $*P < 0.05$ vs. control.

Table 2. *Echocardiographic findings*

	Control	MNC	AM	AM-MNC
LVDd, mm	9.9±0.2	8.3±0.3	7.3±0.2*	6.9±0.3*†
LVDs, mm	8.4±0.3	6.6±0.4	5.8±0.2*	5.1±0.2*
%FS, %	14±1	22±1*	21±1*	26±1*†‡
AWT diastole, mm	1.0±0.2	1.3±0.3*	1.3±0.3*	1.4±0.4*
PWT diastole, mm	1.5±0.5	2.2±0.4	2.1±0.4	2.2±0.4

Values are means ± SE. LVDd, LV diastolic dimension; LVDs, LV systolic dimension; %FS, LV fractional shortening; AWT, anterior wall thickness; PWT, posterior wall thickness. $*P < 0.05$ vs. control; $\dagger P < 0.05$ vs. MNC; $\ddagger P < 0.05$ vs. AM.

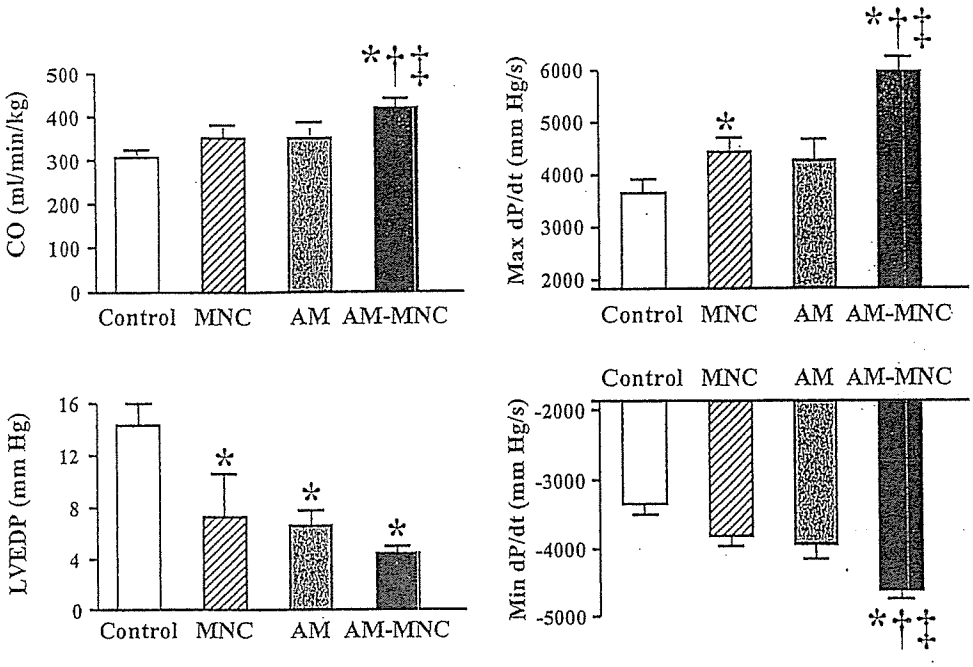

Fig. 2. Effects of AM infusion and MNC transplantation on hemodynamic parameters. CO, cardiac output; LVEDP, LV end-diastolic pressure; Max dP/d*t*, LV maximum change in pressure over time; Min dP/d*t*, LV minimum dP/d*t*. Values are means ± SE. *$P < 0.05$ vs. control; †$P < 0.05$ vs. MNC; ‡$P < 0.05$ vs. AM.

were hardly detected in the AM-MNC group. Semiquantitative analysis demonstrated that the number of TUNEL-positive MNC was significantly lower in the AM-MNC group than in the MNC group. Similarly, the number of caspase-3-positive MNC was significantly lower in the AM-MNC group than in the MNC group. These results suggest that infusion of AM inhibits apoptosis of transplanted MNC.

In vitro, serum starvation induced MNC apoptosis. When incubated in the presence of AM (1×10^{-7} M), the percentage of TUNEL-positive cells decreased significantly (19 ± 1 to 9 ± 1%, $P < 0.05$). However, pretreatment with wortmannin, a PI3-kinase inhibitor, diminished the antiapoptotic effect of AM (17 ± 1%).

Differentiation of MNC into endothelial lineage. Four weeks after transplantation, fluorescence-labeled transplanted cells

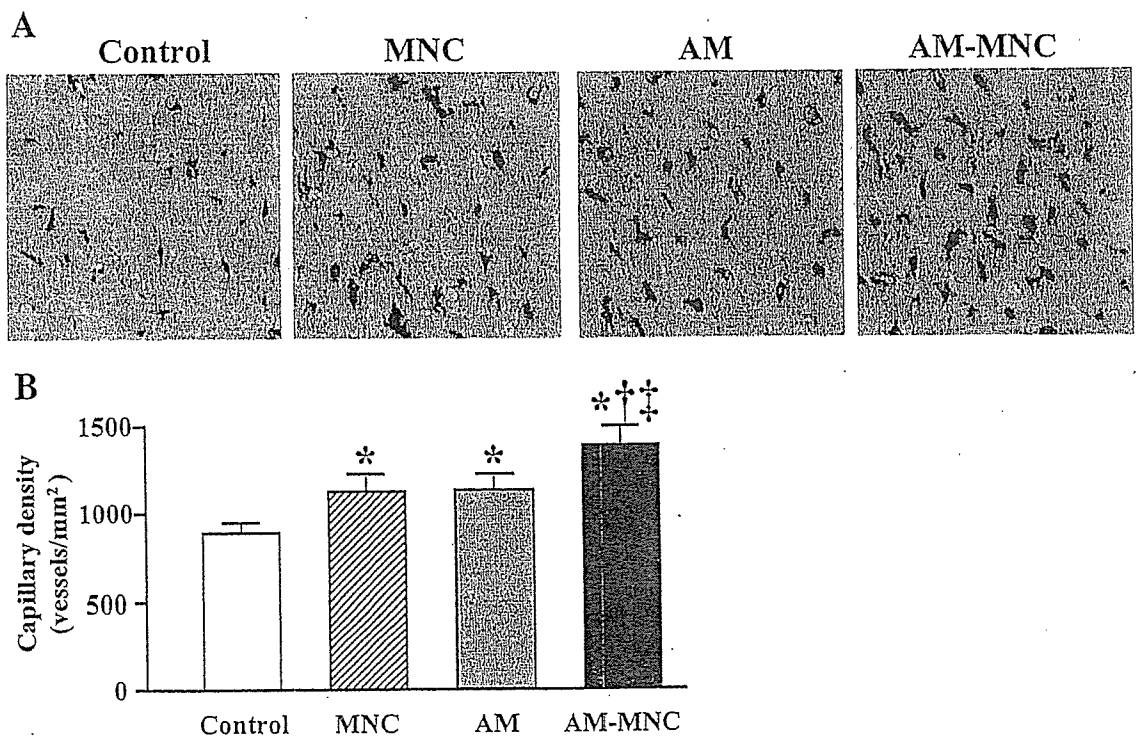

Fig. 3. *A*: representative examples of alkaline phosphatase staining in peri-infarct area. A combination of AM infusion and MNC transplantation markedly induced myocardial neovascularization. Magnification, ×200. *B*: quantitative analysis of capillary density in peri-infarct area. Capillary density in the AM-MNC group was significantly higher than that in the MNC and AM groups. Values are means ± SE. *$P < 0.05$ vs. control; †$P < 0.05$ vs. MNC; ‡$P < 0.05$ vs. AM.

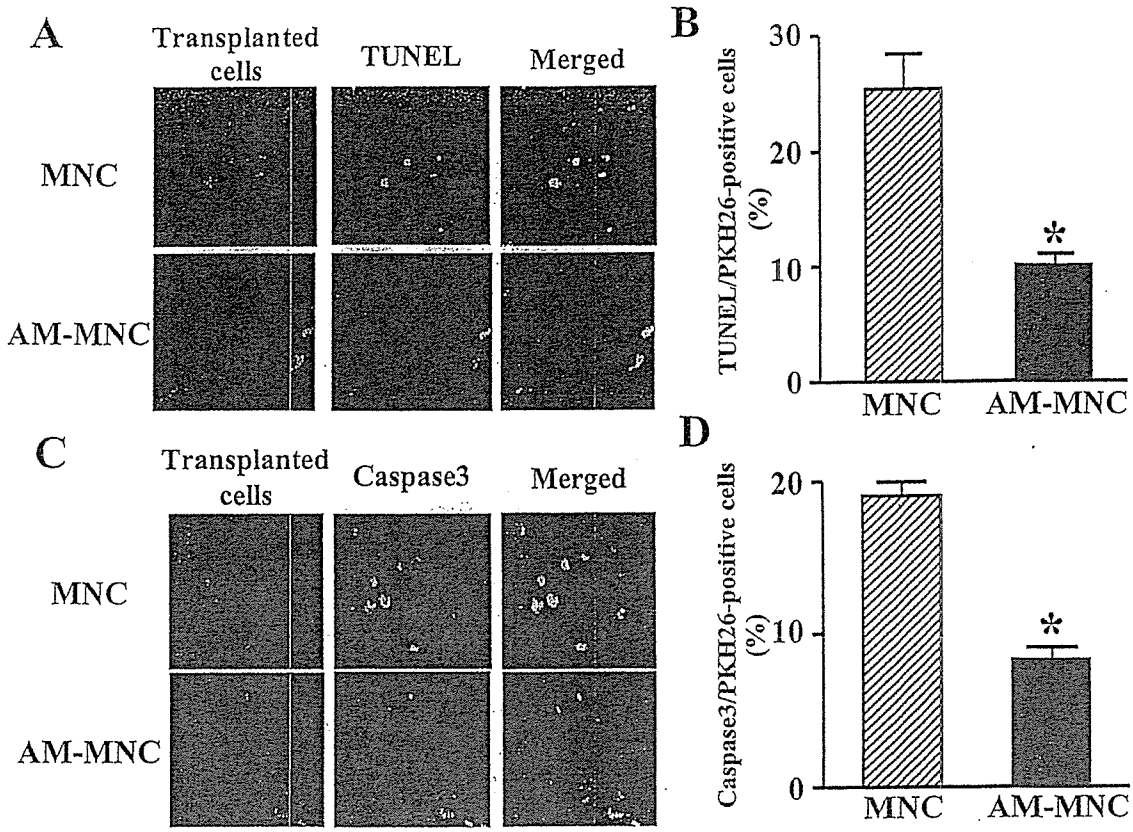

Fig. 4. Detection of transplanted cell apoptosis. *A*: representative photographs of terminal deoxynucleotidyl transferase-mediated dUTP nick end labeling (TUNEL) staining. Red fluorescence (PKH26) marks transplanted MNC; green fluorescence indicates TUNEL-positive cells. TUNEL-positive cells were frequently observed in the MNC group, whereas they were hardly detected in the AM-MNC group. Magnification, ×400. *B*: semiquantitative analysis of TUNEL-positive cells in the PKH26-positive (transplanted) cells. *C*: representative photographs of caspase-3 staining. Red fluorescence (PKH26) marks transplanted MNC; green fluorescence indicates caspase-3-positive cells. *D*: semiquantitative analysis of caspase-3-positive cells in the PKH26-positive cells. Values are means ± SE. $^*P < 0.05$ vs. control.

were more frequently observed in the AM-MNC group than in the MNC group (6.4 ± 0.4 to 3.1 ± 0.2%, $P < 0.05$). Moreover, some of the transplanted cells were positive for UEA-1 lectin in the AM-MNC group (Fig. 5*A*), suggesting differentiation of MNC into vascular endothelial cells. Semiquantitative analysis demonstrated that the number of DAPI/PKH26 double-positive cells (viable transplanted cells) was significantly higher in the AM-MNC group than in the MNC group (Fig. 5*B*). Moreover, the ratio of lectin-positive cells to DAPI/PKH26 double-positive cells was significantly higher in the AM-MNC group than in the MNC group. The ratio of DAPI/PKH26 double-positive cells to lectin-positive cells was small, but significantly higher in the AM-MNC group than in the MNC group (23.9 ± 0.9 to 17.2 ± 0.6%, $P < 0.01$). Transplanted MNC were negative for troponin T or α-smooth muscle actin-positive cells. Some of the transplanted MNC were positive for ED1, a marker of macrophage (data not shown).

DISCUSSION

In the present study, we demonstrated that *1*) infusion of AM enhanced the angiogenic potency of MNC in a rat model of acute myocardial infarction, resulting in decreased infarct size and improved cardiac function. We also demonstrated that *2*) AM induced angiogenesis and inhibited apoptosis of the transplanted MNC. Thus a combination of AM and MNC may have beneficial effects in rats with myocardial infarction, partly through the angiogenic potency of AM itself and through its antiapoptotic effect on MNC.

Bone marrow-derived MNC include a variety of stem and progenitor cells (1, 15, 19), some of which can differentiate into endothelial cells and secrete numerous cytokines and chemokines (6, 9, 10). Earlier studies (6, 9, 10, 23, 25) have shown that autologous bone marrow transplantation induces angiogenesis and improves LV function in animals and humans. However, some patients are refractory to this cell therapy. Thus an approach to augment the angiogenic potency of MNC transplantation is required.

The present study showed that MNC transplantation or AM infusion alone reduced infarct size. A combination of AM infusion and MNC transplantation resulted in further decreases in infarct size and LV chamber size. MNC transplantation or AM administration modestly improved LV function. On the other hand, a combination of MNC and AM significantly improved cardiac performance compared with MNC or AM alone, as indicated by increases in cardiac output, fractional shortening, and LV maximum dP/dt. Earlier studies (6, 9, 10) have reported that MNC transplantation induces therapeutic angiogenesis and preserves LV function through inhibition of cardiomyocyte apoptosis in animal models of myocardial infarction. We have shown that AM infusion during the acute phase of ischemia-reperfusion inhibits apoptosis of cardiomyocytes and produces hemodynamic improvement in an animal

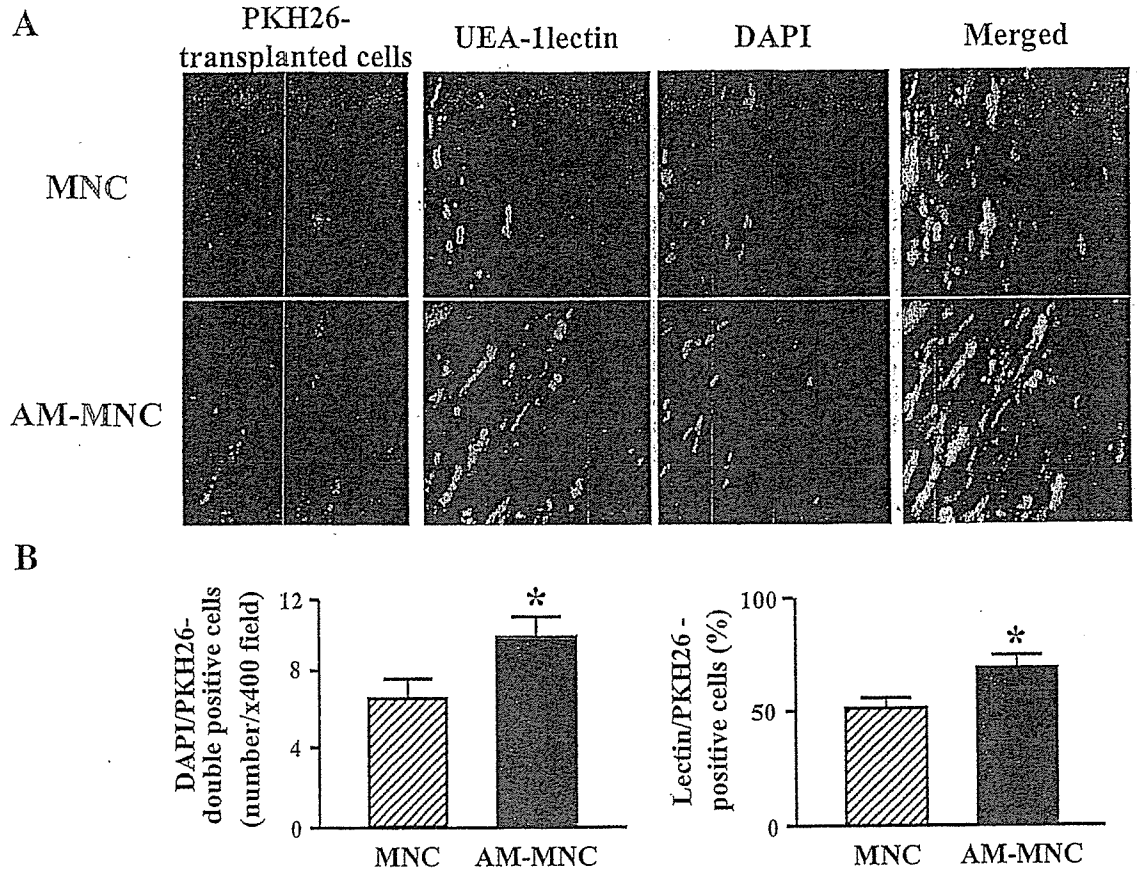

Fig. 5. *A*: representative examples of MNC differentiation into endothelial lineage. Red fluorescence (PKH26) marks transplanted cells; green fluorescence indicates ulex europaeus (UEA)-1 lectin, a marker for vascular endothelial cells. Most of the transplanted cells differentiated into endothelial cells in the AM-MNC group. Magnification, ×400. *B*: quantitative analysis of living transplanted cells and endothelial differentiation. The number of living cells after transplantation was significantly higher in the AM-MNC group than in the MNC group. The ratio of lectin-positive cells to living transplanted cells was significantly higher in the AM-MNC group than in the MNC group. Values are means ± SE. $*P < 0.05$ vs. control. DAPI, 4′,6′-diamidino-2-phenylindole.

study (18). These findings suggest that the reduction of infarct size induced by this combination therapy may be attributable to additive cardioprotective effects of MNC and AM.

The present study showed that AM infusion significantly increased capillary density in ischemic myocardium. Furthermore, AM infusion plus MNC transplantation demonstrated a further increase in capillary density compared with AM or MNC alone. Contribution of transplanted MNC to neovascularization (the ratio of DAPI/PKH26 double-positive cells to lectin-positive cells) was significantly greater in the AM-MNC group than in the MNC group. A recent study (14) has reported that AM promotes proliferation and migration of human umbilical vein endothelial cells and enhances angiogenesis in a murine gel plug assay through the PI3-kinase/Akt pathway. We have also shown that intramuscular administration of AM DNA induces therapeutic angiogenesis in a rabbit model of chronic hindlimb ischemia via activation of Akt (24). These findings suggest that the beneficial effects of combination therapy using AM and MNC may be attributable, in part, to the angiogenic properties of AM itself. Thus it is possible that AM infusion and MNC transplantation induce additive effects on myocardial damage after myocardial infarction. However, it still remains unknown whether AM infusion plus MNC transplantation induces synergetic effects.

An earlier study has demonstrated that ischemia and mechanical stress induce apoptosis of transplanted cells in the early stage after MNC transplantation (9). These results raise the possibility that the angiogenic potency of MNC transplantation is attenuated by MNC apoptosis. Kim et al. (7) have demonstrated that AM inhibits apoptosis of endothelial cells through the PI3-kinase/Akt pathway in vitro. Activation of the PI3-kinase/Akt pathway has been shown to inhibit apoptosis of endothelial progenitor cells and enhance neovascularization (11). In the present study, AM infusion significantly inhibited MNC apoptosis in ischemic tissue. In vitro, we showed that the antiapoptotic effect of AM on MNC was mediated by activation of the PI3-kinase/Akt pathway. Thus AM may enhance the therapeutic potency of MNC transplantation through a direct action of AM on MNC survival. Moreover, immunohistological examination demonstrated that infusion of AM increased the number of lectin-positive (endothelial) cells in transplanted MNC. These findings raise the possibility that AM may enhance differentiation of MNC into the endothelial lineage. Thus AM may directly act on transplanted MNC, which may result in synergetic effects on the ischemic myocardium.

This study includes some study limitations. Although the labeling efficacy of PKH26 has been shown to persist for >8 wk without cell toxicity (3, 4), the used vital marker PKH26

may have some cell toxic effects and cell or membrane fusion can lead to labeling of neighboring cells in the target tissue. Second, the present study demonstrated that AM prolongs MNC survival through the PI3-kinase/Akt pathway and enhances neovascularization in a peri-infarcted area. However, further studies are necessary to examine the effect of AM on MNC differentiation into endothelial cells.

Autologous cell transplantation may be an alternative treatment for ischemic heart disease in the clinical setting. Because their use does not require immunosuppression, the clinical use of MNC for cellular cardiomyoplasty appears to be most advantageous. Administration of AM peptide is simple and relatively noninvasive. We and others (12, 16, 17) have reported the safety of AM infusion in humans. Thus combination therapy using AM infusion and MNC transplantation may be a new therapeutic strategy for the treatment of ischemic heart disease.

In conclusion, infusion of AM enhanced the angiogenic potency of MNC transplantation and improved cardiac function in rats with myocardial infarction. This beneficial effect may be mediated partly by the angiogenic property of AM itself and by its antiapoptotic effect on MNC. Thus combination therapy using AM infusion and MNC transplantation may be a new therapeutic strategy for the treatment of ischemic heart disease.

GRANTS

This work was supported by Ministry of Education, Culture, Sports, Science and Technology Grant-in-Aid for Scientific Research 13470154; Health and Labor Sciences Research Grants nano 001 and genome 005; Ministry of Health, Labor and Welfare Research Grant for Cardiovascular Disease H13C-1 and 16C-6; and grants from New Energy and Industrial Technology Development Organization and the Promotion of Fundamental Studies in Health Science of the Organization for Pharmaceutical Safety and Research of Japan.

REFERENCES

1. Asahara T, Murohara T, Sullivan A, Silver M, van der Zee R, Li T, Witzenbichler B, Schatteman G, and Isner JM. Isolation of putative progenitor endothelial cells for angiogenesis. *Science* 275: 964–967, 1997.
2. Chien YW, Barbee RW, MacPhee AA, Frohlich ED, and Trippodo NC. Increased ANF secretion after volume expansion is preserved in rats with heart failure. *Am J Physiol Regul Integr Comp Physiol* 254: R185–R191, 1988.
3. Fox D, Kouris GJ, Blumofe KA, Heilizer TJ, Husak V, and Greisler HP. Optimizing fluorescent labeling of endothelial cells for tracking during long-term studies of autologous transplantation. *J Surg Res* 86: 9–16, 1999.
4. Gulbins H, Pritisanac A, Anderson I, Uhlig A, Goldemund A, Daebritz S, Meiser B, and Reichart B. Myoblasts for survive 16 weeks after intracardiac transfer and start differentiation. *Thorac Cardiovasc Surg* 51: 295–300, 2003.
5. Hennekens CH. Increasing burden of cardiovascular disease: current knowledge and future directions for research on risk factors. *Circulation* 97: 1095–1102, 1998.
6. Kamihata H, Matsubara H, Nishiue T, Fujiyama S, Tsutsumi Y, Ozono R, Masaki H, Mori Y, Iba O, Tateishi E, Kosaki A, Shintani S, Murohara T, Imaizumi T, and Iwasaka T. Implantation of bone marrow mononuclear cells into ischemic myocardium enhances collateral perfusion and regional function via side supply of angioblasts, angiogenic ligands, and cytokines. *Circulation* 104: 1046–1052, 2001.
7. Kim W, Moon SO, Sung MJ, Kim SH, Lee S, So JN, and Park SK. Angiogenic role of adrenomedullin through activation of Akt, mitogen-activated protein kinase, and focal adhesion kinase in endothelial cells. *FASEB J* 17: 1937–1939, 2003.
8. Kitamura K, Kangawa K, Kawamoto M, Ichiki Y, Nakamura S, Matsuo H, and Eto T. Adrenomedullin: a novel hypotensive peptide isolated from human pheochromocytoma. *Biochem Biophys Res Commun* 192: 553–560, 1993.
9. Kobayashi T, Hamano K, Li TS, Katoh T, Kobayashi S, Matsuzaki M, and Esato K. Enhancement of angiogenesis by the implantation of self bone marrow cells in a rat ischemic heart model. *J Surg Res* 89: 189–195, 2000.
10. Kocher AA, Schuster MD, Szabolcs MJ, Takuma S, Burkhoff D, Wang J, Homma S, Edwards NM, and Itescu S. Neovascularization of ischemic myocardium by human bone-marrow-derived angioblasts prevents cardiomyocyte apoptosis, reduces remodeling and improves cardiac function. *Nat Med* 7: 430–436, 2001.
11. Llevadot J, Murasawa S, Kureishi Y, Uchida S, Masuda H, Kawamoto A, Walsh K, Isner JM, and Asahara T. HMG-CoA reductase inhibitor mobilizes bone marrow-derived endothelial progenitor cells. *J Clin Invest* 108: 399–405, 2001.
12. McGregor DO, Troughton RW, Frampton C, Lynn KL, Yandle T, Richards AM, and Nicholls MG. Hypotensive and natriuretic actions of adrenomedullin in subjects with chronic renal impairment. *Hypertension* 37: 1279–1284, 2001.
13. Messina LM, Podrazik RM, Whitehill TA, Ekhterae D, Brothers TE, Wilson JM, Burkel WE, and Stanley JC. Adhesion and incorporation of lacZ-transduced endothelial cells into the intact capillary wall in the rat. *Proc Natl Acad Sci USA* 89: 12018–12022, 1992.
14. Miyashita K, Itoh H, Sawada N, Fukunaga Y, Sone M, Yamahara K, Yurugi-Kobayashi T, Park K, and Nakao K. Adrenomedullin provokes endothelial Akt activation and promotes vascular regeneration both in vitro and in vivo. *FEBS Lett* 544: 86–92, 2003.
15. Murohara T, Ikeda H, Duan J, Shintani S, Sasaki K, Eguchi H, Onitsuka I, Matsui K, and Imaizumi T. Transplanted cord blood-derived endothelial precursor cells augment postnatal neovascularization. *J Clin Invest* 105: 1527–1536, 2000.
16. Nagaya N, Kyotani S, Uematsu M, Ueno K, Oya H, Nakanishi N, Shirai M, Mori H, Miyatake K, and Kangawa K. Effects of adrenomedullin inhalation on hemodynamics and exercise capacity in patients with idiopathic pulmonary hypertension. *Circulation* 109: 351–356, 2004.
17. Nagaya N, Satoh T, Nishikimi T, Uematsu M, Furuichi S, Sakamaki F, Oya H, Kyotani S, Nakanishi N, Goto Y, Masuda Y, Miyatake K, and Kangawa K. Hemodynamic, renal, and hormonal effects of adrenomedullin infusion in patients with congestive heart failure. *Circulation* 101: 498–503, 2000.
18. Okumura H, Nagaya N, Itoh T, Okano I, Hino J, Mori K, Tsukamoto Y, Ishibashi-Ueda H, Miwa S, Tambara K, Toyokuni S, Yutani C, and Kangawa K. Adrenomedullin infusion attenuates myocardial ischemia/reperfusion injury through the phosphatidylinositol 3-kinase/Akt-dependent pathway. *Circulation* 109: 242–248, 2004.
19. Rafii S and Lyden D. Therapeutic stem and progenitor cell transplantation for organ vascularization and regeneration. *Nat Med* 9: 702–712, 2003.
20. Sata M, Kakoki M, Nagata D, Nishimatsu H, Suzuki E, Aoyagi T, Sugiura S, Kojima H, Nagano T, Kangawa K, Matsuo H, Omata M, Nagai R, and Hirata Y. Adrenomedullin and nitric oxide inhibit human endothelial cell apoptosis via a cyclic GMP-independent mechanism. *Hypertension* 36: 83–88, 2000.
21. Schiller NB, Shah PM, Crawford M, DeMaria A, Devereux R, Feigenbaum H, Gutgesell H, Reichek N, Sahn D, Schnittger I, Silverman NH, and Tajik AJ. Recommendations for quantitation of the left ventricle by two-dimensional echocardiography. American Society of Echocardiography Committee on Standards, Subcommittee on Quantitation of Two-Dimensional Echocardiograms. *J Am Soc Echocardiogr* 2: 358–367, 1989.
22. Shiojima I and Walsh K. Role of Akt signaling in vascular homeostasis and angiogenesis. *Circ Res* 90: 1243–1250, 2002.
23. Strauer BE, Brehm M, Zeus T, Kostering M, Hernandez A, Sorg RV, Kogler G, and Wernet P. Repair of infarcted myocardium by autologous intracoronary mononuclear bone marrow cell transplantation in humans. *Circulation* 106: 1913–1918, 2002.
24. Tokunaga N, Nagaya N, Shirai M, Tanaka E, Ishibashi-Ueda H, Harada-Shiba M, Kanda M, Ito T, Shimizu W, Tabata Y, Uematsu M, Nishigami K, Sano S, Kangawa K, and Mori H. Adrenomedullin gene transfer induces therapeutic angiogenesis in a rabbit model of chronic hind limb ischemia: benefits of a novel nonviral vector, gelatin. *Circulation* 109: 526–531, 2004.
25. Tse HF, Kwong YL, Chan JK, Lo G, Ho CL, and Lau CP. Angiogenesis in ischaemic myocardium by intramyocardial autologous bone marrow mononuclear cell implantation. *Lancet* 361: 47–49, 2003.